HEAT TRANSFER ANALYSIS OF JOHNSON-SEGALMAN FLUID IN A TAPERED ASYMMETRIC CHANNEL

Student Name: Zulfiqar Ali
Enrollment No: 01-248202-012
Supervised by Dr. Jafar Hasnain

A thesis submitted in fulfilment of the requirements for the award of degree of Masters of Science (Mathematics)

Department of Computer Science

BAHRIA UNIVERSITY ISLAMABAD

SESSION(2020-2022)

Approval of Examination

Scholar Name: Zulfiqar Ali
Registration Number: 71103
Enrollment: 01-248202-012
Program of Study: MS Mathematics

Thesis Title: Heat Transfer Analysis of Johnson-Segalman Fluid in A tapered Asymmetric Channel

It is to certify that the above scholar's thesis has been completed to my satisfaction and, to my belief, its standard is appropriate for submission for examination. I have also conducted plagiarism test of this thesis using HEC prescribed software and found similarity index 17%. that is within the permissible limit set by the HEC for the MS/M. Phil degree thesis. I have also found the thesis in a format recognized by the BU for the MS/M.Phil thesis.

Supervisor Name: Dr. Jafar Hasnain

Supervisor Signature:

Date:

Author's Declaration

I, Zulfiqar Ali hereby state that my MS/M.Phil thesis titled is my own work and has not been submitted previously by me for taking any degree from Bahria university or anywhere else in the country/world. At any time if my statement is found to be incorrect even after my graduation, the University has the right to withdraw/cancel my MS/M.Phil degree.

Scholar signature: _____

Name of Scholar: ZULFIQAR ALI

Date: 08-10- 2022

Plagiarism Undertaking

I, Zulfiqar Ali solemnly declare that research work presented in the thesis titled" Heat Transfer Analysis of Johnson-Segalman Fluid in A tapered Asymmetric Channel" is solely my research work with no significant contribution from any other person. Small contribution / help wherever taken has been duly acknowledged and that complete thesis has been written by me. I understand the zero-tolerance policy of the HEC and Bahria University towards plagiarism. Therefore, I as an Author of the above titled thesis declare that no portion of my thesis has been plagiarized and any material used as reference is properly referred / cited.

I undertake that if I am found guilty of any formal plagiarism in the above titled thesis even after award of MS/M.Phil degree, the university reserves the right to withdraw / revoke my MS/M.Phil degree and that HEC and the University has the right to publish my name on the HEC / University website on which names of scholars are placed who submitted plagiarized thesis

Name of Scholar: ZULFIQAR ALI

Date: 08-10- 2022

Dedication

Dedicated to my Beloved Parents and Respected Supervisor

Acknowledgments

All praises to **Almighty Allah**, the creator of all the creatures in the universe, who has created us in the structure of human beings as the best creature. Many thanks to Him, who created us as a muslim and blessed us with knowledge to differentiate between right and wrong. Many many thanks to Him as he blessed us with the Holy Prophet, **Hazrat Muhammad (Sallallahu Alaihay Wa'alihi wasalam)** for Whom the whole universe is created. He (Sallallahu Alaihay Wa'alihi wasalam) brought us out of darkness and enlightened the way to heaven.

I express my heart-felt gratitude to my supervisor **Dr. Jafar Hasnain** for his passionate interest, superb guidance, and inexhaustible inspiration throughout this investigation. His textural and verbal criticism enable me in formatting this manuscript. My debt of gratitude goes to all my respectable teachers especially **Prof. Dr. M. Ramzan**, **Dr. Rizwan ul Haq** and **Dr. Muhammad Yousaf Rafiq** for their inspirational guidance. May Almighty Allah shower His choicest blessings and prosperity on all those who assisted me in any way during completion of my thesis. I would like to express my special thanks to **Dr. Muhammad Ismail** and **Sarang Khan** they supported me in every situation of my Career. And I am also thankful to my seniors Phd students who were always remained helpful to me **Nomana Abid** and my friend **Iqra Rauf**. May Allah shower His blessings upon them more than enough.

Abstract

This study presents a theoretical thermal analysis for the peristaltic transportation of electrically conducting Johnson-Segalman liquid through a two-dimensional asymmetric tapered following the propagation of sinusoidal wave trains with dissimilar phases. The impact of viscous dissipation is also deliberated in the modeling. Mathematical modeling is carried out by making use of lubrication approximation theory. The fundamental equations of the Johnson Segalman fluid are solved by regular perturbation technique and the expressions for velocity, energy and stream functions are attained. The impact of various embedded parameters on the flow fields is illustrated graphically and discussed in detail. The significant outcomes of the current analysis are that the liquid velocity declined with the higher values of magnetic parameter and enhances with Johnson-Segalman liquid parameter. Pressure rise improves in the augmented pumping portion with the magnetic parameter.

TABLE OF CONTENTS

AUTHOR'S DECLARATION ..... **ii**
PLARIGISIM UNDERTAKING ..... **iii**
DEDICATION ..... **iv**
ACKNOWLDGEMENTS ..... **v**
ABSTRACT ..... **vi**
LIST OF FIGURES ..... **ix**
LIST OF SYMBOLS ..... **xi**
CHAPTER 1 INTRODUCTION **1**
1.1 Overview 1
1.2 Fluid 1
1.3 Fluid Rheology 1
1.3.1 Newtonian fluids (NF) 1
1.3.2 Non-Newtonian fluid (NNF) 2
1.4 Peristaltic flow 2
1.4.1 Flowing Regions 2
1.4.2 Trapping phenomenon 3
1.5 Dimensionless numbers 3
1.6 Governing equations 6
1.7 Tensor equation of Johnson-Segalman (JS) fluid 7
1.8 Solution method 11
CHAPTER 2 LITERATURE REVIEW **13**
2.1 Overview 13

2.2 Literature Review 13
CHAPTER 3 A TAPERED ASYMMETRIC CHANNEL WITH NONLINEAR PERISTALTIC MOTION OF JOHNSON-SEGALMAN FLUID 17
3.1 Overview 17
3.2 Mathematical formulation 17
3.4 Graphical results and discussion 23
CHAPTER 4 HEAT TRANSFER ANALYSIS OF JOHNSON-SEGALMAN FLUID IN A TAPERED ASYMMETRIC CHANNEL 33
4.1 Overview 33
4.2 Problem Statement 33
4.3. Solution of the problem 37
4.4 Discussion of the findings 41
CHAPTER 5 CONCLUSION AND FUTURE WORK 50
5.1 Conclusion 50
5.2 Future work 51
APPENDIX 52
REFERENCES 55

LIST OF FIGURES

Figure 2.1: Peristalsis mechanism 2
Figure 3.1: Problems geometry 18
Figure 3.2: Upshot of a on pressure 25
Figure 3.3: Upshot of k on pressure 25
Figure 3.4: Upshot of We on pressure 26
Figure 3.5: Upshot of ϕ on pressure 26
Figure 3.6: Upshot of e on pressure 27
Figure 3.7: Upshot of η on pressure 27
Figure 3.8: Upshot of a on axial velocity 28
Figure 3.9: Upshot of e on axial velocity 28
Figure 3.10: Upshot of γ_1 on axial velocity 29
Figure 3.11: Upshot of k on axial velocity 29
Figure 3.12: Upshot of We on axial velocity 30
Figure 3.13: Upshot of Q on axial velocity 30
Figure 3.14: Streamlines for various values of (a) $a = 0$,(b) $a = 0.3$ 31
Figure 3.15: Streamlines for various values of (a) $Q = 1.5$,(b) $Q = 1.6$ 31
Figure 3.16: Streamlines for various values of (a) $We = 0$,(b) $We = 0.6$ 32
Figure 4.1: Problems geometry 34
Figure 4.2(a): Effects of M on axial velocity 43
Figure 4.2(b): Effects of β on axial velocity 43
Figure 4.2(c): Effects of We on axial velocity 44
Figure 4.2(d): Effects of e on axial velocity 44
Figure 4.3(a): Effects of Br on temperature 45
Figure 4.3(b): Effects of Rd on temperature 45

Figure 4.3(c): Effects of We on temperature.....46
Figure 4.4(a): Effects of M on pressure.....46
Figure 4.4(b): Effects of β on pressure.....47
Figure 4.4(c): Effects of e on pressure 47
Figure 4.4(d): Effects of We on pressure.....48
Figure 4.5: Streamlines for various values of (a) $M = 1$ (b) $M = 2$ 48
Figure 4.6: Streamlines for various values of (a) $Q = 1.2$, (b) $Q = 1.4$ 49
Figure 4.7: Streamlines for various values of (a) $We = 0$, (b) $We = 0.2$ 49

LIST OF SYMBOLS

d	channel half-width
k'	non-uniform parameter
c	wave speed
$\widehat{U},\widehat{V}$	laboratory frame velocity components
t	Time
T_0, T_1	temperature at upper and lower wall
a_1, a_2	amplitude of wave at upper and lower wall
u, v	wave frame velocity components
x, y	space coordinates in wave frame
p	Pressure
m	Relaxation time
μ,η	dynamic viscosities
λ	Wavelength
B_0	strength of magnetic field
B_r	Brinkman number
e	slip parameter
Pr	Prandtl number
Δp	pressure rise
$\widehat{Q}$	time average of the flux
M	magnetic number
C_p	specific heat
Ec	Eckert Number
Re	Reynold's number
σ^*	Stefan - Boltzmann constant

$\widehat{D},\widehat{W}$	symmetric and skew-symmetric
ψ	dimensionless stream function
τ	Cauchy stress tensor
δ	Wavenumber
ρ	fluid density
ξ	thermal conductivity constant
q_r	radiative heat flux
β	velocity slip parameter
We	Weissenberg number
k^*	mean absorption coefficient
ϕ	Phase difference
σ	Electrical Conductivity
	Abbreviations
JS	Johnson-Segalman
PT	Peristaltic transport
NF	Newtonian fluid
NNF	Non-Newtonian fluid
PDE	Partial differential equation
ODE	Ordinary differentials equation

CHAPTER 1

INTRODUCTION

1.1 Overview

This chapter is intended to provide basic fluid mechanics ideas as well as definitions of numerous dimensionless numbers and equations in order to explain the flow analysis presented in this study.

1.2 Fluid

When a shearing stress is applied to a fluid, the individual particles, no matter how small, deform constantly.

1.3 Fluid Rheology

The term "rheology" refers to the study of fluid movements and deformation in response to stress. Shear stress has a very small impact on fluids that flow incompressible. Real fluid is defined as a fluid with at least some viscosity. The truth is that every fluid found or existing in the environment is classified as a real fluid. For instance, water. Real fluid can be further divided into the following categories:

1.3.1 Newtonian fluids (NF)

The relation between strain and stress rate is linear in an NF. NF are those that follow Newton's law of viscosity. According to this rule, shear stress is directly but inversely related to deformation rate.

Mathematically,

$$\tau \propto \frac{\partial u}{\partial y},$$

$$\tau = \mu \frac{\partial u}{\partial y}, \tag{1.1}$$

where μ is the dynamic viscosity of the liquid, which is constant for NF at a given temperature and pressure. Examples of NF are air and water.

1.3.2 Non-Newtonian fluid (NNF)

Any liquid in which relation between shear stress and the rate of deformation is direct but not linearly proportional to the rate of deformation is referred to as NNF. Mathematically,

$$\tau = k\left(\frac{\partial u}{\partial y}\right)^{n}, \tag{1.2}$$

where n signifies the flow actions index and k indicates the consistency index.

1.4 Peristaltic flow

Peristalsis is a series of wave-like muscular cramps that migrate to the food separate processing station in the digestive tracks. The Peristalsis process begins in the esophagus when a bolus meal is consumed.

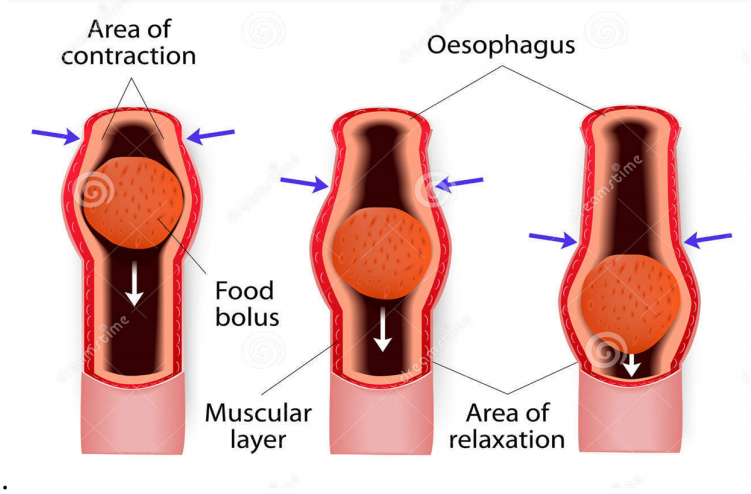

Figure 1. 1: Peristalsis mechanism

1.4.1 Flowing Regions

Peristaltic movement is discretized interested in four kinds of movement areas or quadrants known as unfavorable pressure if pressure increase $(\Delta P > 0)$ and favorable

pressure gradient if pressure rise $(\Delta P < 0)$. These zones are defined by the pressure variation with the time mean flow rate.

i. Peristaltic pumping

The stream rate is positive in this case $(Q > 0)$, However, the increase in pressure is unfavorable $(\Delta p > 0)$.

ii. Retrograde pumping

The stream rate is inefficient. $(Q < 0)$, and the pressure rise is adverse $(\Delta p > 0)$.

iii. Co-pumping

Co-pumping depicts a movement in which the time mean flow is negative with $(\Delta P < 0)$

iv. Enhanced pumping

The stream rate is positive $(Q < 0)$ in this scenario, yet the pressure rise is neither unfavorable nor beneficial. In other terms $\Delta p = 0$.

1.4.2 Trapping phenomenon

A fundamental physical fact of peristalsis is trapping. It is based on the streamline's contours. A bolus of fluid may occasionally be contained in closed streamlines, creating a circulating area, instead of flowing in the direction of the peristaltic wall. The trapped bolus illustrates the peristalsis flow trapping phenomenon by moving with the wave in the flow.

1.5 Dimensionless numbers

This segment is intended to provide an explanation and definition of some of the basic parameters involved in fluid flow

i. Reynolds number

It is a non-dimensional quantity that can be used in fluid dynamics to predict fluid flow regimes in a range of flow patterns. In fluid mechanics, it can be used for a variety of purposes. It is denoted by the letter Re, and written as

$$\mathrm{Re} = \frac{\rho c d}{\mu}, \tag{1.3}$$

where ρ, c, d and μ are density, width, and dynamic viscosity respectively.

ii. Wave number

The wavelength to channel width ratio is known as the wave number. The Greek letter δ is used to represent it.

$$\delta = \frac{d}{\lambda}, \tag{1.4}$$

where d and λ are width of channel and wavelength

iii. Weissenberg Number

In viscoelastic flow analysis, We is a dimensionless number.

$$We = \frac{mc}{d}, \tag{1.5}$$

where m is relaxation time parameter.

iv. Brinkmann Number

It is a dimensionless number used in polymer manufacturing to represent heat transmission from a wall to a moving viscous fluid. It expresses the proportion of heat generated by viscous fluids to heat generated by external sources. The greater the value, the less heat is transmitted by viscous dissipation, causing temperature to rise. This is calculated as follows:

$$Br = \mathrm{Pr}\, Ec, \tag{1.6}$$

v. Eckert Number

In continuum mechanics, Eckert number is a dimensionless number which shows the relation amid temperature and kinetic energy to demonstrate viscous dissipation

$$Ec = \frac{c^2}{C_p \Delta T}, \tag{1.7}$$

where C_p and ΔT are specific heat and change in temperature.

vi. Hartmann Number

An electrically conducting fluid experiences the Lorentz force under the effects of applied magnetic field. The study of these fluids is known as magnetohydrodynamics (MHD). The Lorentz force, which is a repulsive force, slows the velocity field. It is represented as a body force in the momentum equation. The Hartmann number is a non-dimensional quantity obtained by dividing the Lorentz force by the viscous force. The Hartmann number can so be written as

$$M = \sqrt{\frac{\sigma}{\mu}} B_0 d, \tag{1.8}$$

where σ is electrical conductivity parameter

vii. Prandtl Number

It is the momentum-to-thermal-diffusivity ratio, it is dimensionless number which can be written as mathematically

$$\Pr = \frac{\mu C_p}{\xi}, \tag{1.9}$$

where ξ is thermal conductivity constant.

viii. Radiation Parameter

The relation among thermal radiation and conduction heat transfer is defined by the radiation parameter.

$$Rd = \frac{16 T_0^3 \sigma^*}{3 k^* \xi}, \tag{1.10}$$

where σ^*, T_0 and k^* represent the Stefan - Boltzmann constant, energy at upper wall, and mean absorption coefficient respectively.

1.6 Governing equations

The study of fluid behavior based on some important fluid mechanics laws. These laws are as follows [18]:

i. Continuity Equation

The mass conservation law is quantitatively stated in the continuity equation. It is as follows for compressible flows.

$$\frac{\partial \rho}{\partial t} + \nabla.\left(\rho V\right) = 0, \tag{1.11}$$

where t denotes time. The density of incompressible flows remains constant, hence the continuity equation becomes

$$\nabla.V = 0\,, \tag{1.12}$$

ii. Momentum Equation

For magnetohydrodynamic flow, the appropriate equation of motion that illustrates the law of conservation of momentum is as follows:

$$\frac{d\boldsymbol{V}}{dt} = \frac{1}{\rho} div\boldsymbol{\tau} + \frac{1}{\rho}\mathbf{f}, \tag{1.13}$$

The Cauchy stress tensor is denoted by $\boldsymbol{\tau} = \widehat{\boldsymbol{S}} - \widehat{\boldsymbol{p}}\widehat{\boldsymbol{I}} + 2\mu\widehat{\boldsymbol{D}}$, in the above expression. Where d/dt , $\widehat{\boldsymbol{p}}, \widehat{\boldsymbol{I}}, \widehat{\boldsymbol{S}}, \widehat{\boldsymbol{D}}$,and $\boldsymbol{V}$ are material derivative, pressure, identity, extra stress tensors, Symmetric part of velocity gradient, and velocity vector respectively. The term f represents the body force. It reflects the Lorentz force that develops because of a change in magnetic field in the current thesis.

So,

$$\mathbf{f} = \boldsymbol{J} \times \boldsymbol{B}, \tag{1.14}$$

In which $\boldsymbol{B} = \boldsymbol{B}_o$ represent applied magnetic field.

iii. Energy Equation

The first law of thermodynamics is where the energy equation is obtained, and it applies the energy conservation law.

$$\frac{dT}{dt} = \frac{1}{\rho C_p}\boldsymbol{\tau}\cdot\widehat{\boldsymbol{L}} + \frac{\xi}{\rho C_p}\nabla^2 T - \frac{1}{\rho C_p}\nabla\cdot\boldsymbol{q}_r, \tag{1.15}$$

where $T, \widehat{\boldsymbol{L}}$ and $\boldsymbol{q}_r$ are temperature velocity gradient and thermal radiation respectively.

1.7 Tensor equation of Johnson-Segalman (JS) fluid

The following expression describes the Cauchy stress tensor τ for the JS fluid model.

$$\boldsymbol{\tau} = \widehat{\boldsymbol{S}} - \widehat{\boldsymbol{p}}\widehat{\boldsymbol{I}} + 2\mu\widehat{\boldsymbol{D}}, \tag{1.16}$$

In which extra stress tensor $\widehat{\boldsymbol{S}}$ satisfies.

$$\widehat{\boldsymbol{S}} + m\left[\frac{d\widehat{\boldsymbol{S}}}{dt'} + \widehat{\boldsymbol{S}}\left(\widehat{\boldsymbol{W}} - e\widehat{\boldsymbol{D}}\right)^T + \left(\widehat{\boldsymbol{W}} - e\widehat{\boldsymbol{D}}\right)\widehat{\boldsymbol{S}}\right] = 2\eta\widehat{\boldsymbol{D}}, \tag{1.17}$$

$$\widehat{\boldsymbol{D}} = \frac{1}{2}\left[\widehat{\boldsymbol{L}} + \widehat{\boldsymbol{L}}^T\right], \qquad \widehat{\boldsymbol{W}} = \frac{1}{2}\left[\widehat{\boldsymbol{L}} - \widehat{\boldsymbol{L}}^T\right], \qquad \widehat{\boldsymbol{L}} = grad\boldsymbol{V}, \tag{1.18}$$

Notice that the current model diminishes to the fluid model given by Maxwell for e=1 and we attain the basic NS model for $\mu = 0$.

The velocity for 2-D unsteady flow is specified as:

$$\boldsymbol{V} = \left[\widehat{U}\left(\widehat{X}, \widehat{X}, t'\right), \widehat{V}\left(\widehat{X}, \widehat{Y}, t'\right), 0\right], \tag{1.19}$$

The aforementioned equation allows one to write down

$$\widehat{\boldsymbol{L}} = grad\boldsymbol{V} = \begin{bmatrix} \frac{\partial\widehat{U}}{\partial\widehat{X}} & \frac{\partial\widehat{U}}{\partial\widehat{Y}} & 0 \\ \frac{\partial\widehat{V}}{\partial\widehat{X}} & \frac{\partial\widehat{V}}{\partial\widehat{Y}} & 0 \\ 0 & 0 & 0 \end{bmatrix}, \ \widehat{\boldsymbol{L}}^T = \left(grad\boldsymbol{V}\right)^T = \begin{bmatrix} \frac{\partial\widehat{U}}{\partial\widehat{X}} & \frac{\partial\widehat{V}}{\partial\widehat{X}} & 0 \\ \frac{\partial\widehat{U}}{\partial\widehat{Y}} & \frac{\partial\widehat{V}}{\partial\widehat{Y}} & 0 \\ 0 & 0 & 0 \end{bmatrix}, \tag{1.20}$$

$$\widehat{\boldsymbol{D}} = \frac{1}{2}\left[\widehat{L} + \widehat{L}^{T}\right] = \frac{1}{2}\begin{bmatrix} 2\dfrac{\partial \widehat{U}}{\partial \widehat{X}} & \dfrac{\partial \widehat{U}}{\partial \widehat{Y}} + \dfrac{\partial \widehat{V}}{\partial \widehat{X}} & 0 \\ \dfrac{\partial \widehat{V}}{\partial \widehat{X}} + \dfrac{\partial \widehat{U}}{\partial \widehat{Y}} & 2\dfrac{\partial \widehat{V}}{\partial \widehat{Y}} & 0 \\ 0 & 0 & 0 \end{bmatrix}$$

$$= \begin{bmatrix} \dfrac{\partial \widehat{U}}{\partial \widehat{X}} & \left[\dfrac{1}{2}\dfrac{\partial \widehat{U}}{\partial \widehat{Y}} + \dfrac{1}{2}\dfrac{\partial \widehat{V}}{\partial \widehat{X}}\right] & 0 \\ \left[\dfrac{1}{2}\dfrac{\partial \widehat{V}}{\partial \widehat{X}} + \dfrac{1}{2}\dfrac{\partial \widehat{U}}{\partial \widehat{Y}}\right] & \dfrac{\partial \widehat{V}}{\partial \widehat{Y}} & 0 \\ 0 & 0 & 0 \end{bmatrix}, \tag{1.21}$$

$$\widehat{\boldsymbol{W}} = \frac{1}{2}\left[\widehat{\boldsymbol{L}} - \widehat{\boldsymbol{L}}^{T}\right] = \frac{1}{2}\begin{bmatrix} 0 & \dfrac{\partial \widehat{U}}{\partial \widehat{Y}} - \dfrac{\partial \widehat{V}}{\partial \widehat{X}} & 0 \\ \dfrac{\partial \widehat{V}}{\partial \widehat{X}} - \dfrac{\partial \widehat{U}}{\partial \widehat{Y}} & 0 & 0 \\ 0 & 0 & 0 \end{bmatrix}$$

$$= \begin{bmatrix} 0 & \left[\dfrac{1}{2}\dfrac{\partial \widehat{U}}{\partial \widehat{Y}} - \dfrac{1}{2}\dfrac{\partial \widehat{V}}{\partial \widehat{X}}\right] & 0 \\ \left[\dfrac{1}{2}\dfrac{\partial \widehat{V}}{\partial \widehat{X}} - \dfrac{1}{2}\dfrac{\partial \widehat{U}}{\partial \widehat{Y}}\right] & 0 & 0 \\ 0 & 0 & 0 \end{bmatrix}, \tag{1.22}$$

Using Eqs. (1.20) - (1.22) in Eq. (1.17)

$$\left(\widehat{\boldsymbol{W}}-e\widehat{\boldsymbol{D}}\right)=\begin{bmatrix} -e\dfrac{\partial\widehat{U}}{\partial\widehat{X}} & \dfrac{1}{2}\left[\dfrac{\partial\widehat{U}}{\partial\widehat{Y}}-e\dfrac{\partial\widehat{U}}{\partial\widehat{Y}}\right]+\dfrac{1}{2}\left[e\dfrac{\partial\widehat{V}}{\partial\widehat{X}}-\dfrac{\partial\widehat{V}}{\partial\widehat{X}}\right] & 0 \\ \dfrac{1}{2}\left[\dfrac{\partial\widehat{V}}{\partial\widehat{X}}-e\dfrac{\partial\widehat{V}}{\partial\widehat{X}}\right]+\dfrac{1}{2}\left[e\dfrac{\partial\widehat{U}}{\partial\widehat{Y}}-\dfrac{\partial\widehat{U}}{\partial\widehat{Y}}\right] & -e\dfrac{\partial\widehat{V}}{\partial\widehat{Y}} & 0 \\ 0 & 0 & 0 \end{bmatrix},$$

$$\left(\widehat{\boldsymbol{W}}-e\widehat{\boldsymbol{D}}\right)^{T}=\begin{bmatrix} -e\dfrac{\partial\widehat{U}}{\partial\widehat{X}} & \dfrac{1}{2}\left[\dfrac{\partial\widehat{V}}{\partial\widehat{X}}-e\dfrac{\partial\widehat{V}}{\partial\widehat{X}}\right]+\dfrac{1}{2}\left[e\dfrac{\partial\widehat{U}}{\partial\widehat{Y}}-\dfrac{\partial\widehat{U}}{\partial\widehat{Y}}\right] & 0 \\ \dfrac{1}{2}\left[\dfrac{\partial\widehat{U}}{\partial\widehat{Y}}-e\dfrac{\partial\widehat{U}}{\partial\widehat{Y}}\right]+\dfrac{1}{2}\left[e\dfrac{\partial\widehat{V}}{\partial\widehat{X}}-\dfrac{\partial\widehat{V}}{\partial\widehat{X}}\right] & -e\dfrac{\partial\widehat{V}}{\partial\widehat{Y}} & 0 \\ 0 & 0 & 0 \end{bmatrix},$$

(1.23)

$$2\eta\widehat{\boldsymbol{D}}=\begin{bmatrix} 2\eta\dfrac{\partial\widehat{U}}{\partial\widehat{X}} & \left[\eta\dfrac{\partial\widehat{U}}{\partial\widehat{Y}}+\eta\dfrac{\partial\widehat{V}}{\partial\widehat{X}}\right] & 0 \\ \left[\eta\dfrac{\partial\widehat{V}}{\partial\widehat{X}}+\eta\dfrac{\partial\widehat{U}}{\partial\widehat{Y}}\right] & 2\eta\dfrac{\partial\widehat{V}}{\partial\widehat{X}} & 0 \\ 0 & 0 & 0 \end{bmatrix}, \tag{1.24}$$

$$\widehat{\boldsymbol{S}}+m\left[\frac{d\widehat{\boldsymbol{S}}}{dt}+\widehat{\boldsymbol{S}}\left[\begin{bmatrix} -e\dfrac{\partial\widehat{U}}{\partial\widehat{X}} & \dfrac{1}{2}\left[\dfrac{\partial\widehat{U}}{\partial\widehat{Y}}-e\dfrac{\partial\widehat{U}}{\partial\widehat{Y}}\right]+\dfrac{1}{2}\left[e\dfrac{\partial\widehat{V}}{\partial\widehat{X}}-\dfrac{\partial\widehat{V}}{\partial\widehat{X}}\right] & 0 \\ \dfrac{1}{2}\left[\dfrac{\partial\widehat{V}}{\partial\widehat{X}}-e\dfrac{\partial\widehat{V}}{\partial\widehat{X}}\right]+\dfrac{1}{2}\left[e\dfrac{\partial\widehat{U}}{\partial\widehat{Y}}-\dfrac{\partial\widehat{U}}{\partial\widehat{Y}}\right] & -e\dfrac{\partial\widehat{V}}{\partial\widehat{Y}} & 0 \\ 0 & 0 & 0 \end{bmatrix}+\begin{bmatrix} -e\dfrac{\partial\widehat{U}}{\partial\widehat{X}} & \dfrac{1}{2}\left[\dfrac{\partial\widehat{V}}{\partial\widehat{X}}-e\dfrac{\partial\widehat{V}}{\partial\widehat{X}}\right]+\dfrac{1}{2}\left[e\dfrac{\partial\widehat{U}}{\partial\widehat{Y}}-\dfrac{\partial\widehat{U}}{\partial\widehat{Y}}\right] & 0 \\ \dfrac{1}{2}\left[\dfrac{\partial\widehat{U}}{\partial\widehat{Y}}-e\dfrac{\partial\widehat{U}}{\partial\widehat{Y}}\right]+\dfrac{1}{2}\left[e\dfrac{\partial\widehat{V}}{\partial\widehat{X}}-\dfrac{\partial\widehat{V}}{\partial\widehat{X}}\right] & -e\dfrac{\partial\widehat{V}}{\partial\widehat{Y}} & 0 \\ 0 & 0 & 0 \end{bmatrix}\right]\right]$$

$$=\begin{bmatrix} 2\eta\dfrac{\partial\widehat{U}}{\partial\widehat{Y}} & \left[\eta\dfrac{\partial\widehat{U}}{\partial\widehat{Y}}+\eta\dfrac{\partial\widehat{V}}{\partial\widehat{X}}\right] & 0 \\ \left[\eta\dfrac{\partial\widehat{V}}{\partial\widehat{X}}+\eta\dfrac{\partial\widehat{U}}{\partial\widehat{Y}}\right] & 2\eta\dfrac{\partial\widehat{V}}{\partial\widehat{Y}} & 0 \\ 0 & 0 & 0 \end{bmatrix}, \tag{1.25}$$

$$2\mu\widehat{\boldsymbol{D}}=\begin{bmatrix} 2\mu\dfrac{\partial\widehat{U}}{\partial\widehat{X}} & \left[\mu\dfrac{\partial\widehat{U}}{\partial\widehat{Y}}+\mu\dfrac{\partial\widehat{V}}{\partial\widehat{X}}\right] & 0 \\ \left[\mu\dfrac{\partial\widehat{V}}{\partial\widehat{X}}+\mu\dfrac{\partial\widehat{U}}{\partial\widehat{Y}}\right] & 2\mu\dfrac{\partial\widehat{V}}{\partial\widehat{Y}} & 0 \\ 0 & 0 & 0 \end{bmatrix}, \tag{1.26}$$

Using Eqs (1.25) -(1.26) in (1.16), we get Cauchy stress tensor for JS fluid.

$$\boldsymbol{\tau}_{\widehat{X}\widehat{X}}=\widehat{\boldsymbol{S}}_{\widehat{X}\widehat{X}}-\widehat{P}+2\mu\frac{\partial\widehat{U}}{\partial\widehat{X}},\ \ \boldsymbol{\tau}_{\widehat{X}\widehat{Y}}=\boldsymbol{\tau}_{\widehat{Y}\widehat{X}}=\widehat{\boldsymbol{S}}_{\widehat{X}\widehat{Y}}+\mu\left[\frac{\partial\widehat{U}}{\partial\widehat{Y}}+\frac{\partial\widehat{V}}{\partial\widehat{X}}\right],$$
$$\boldsymbol{\tau}_{\widehat{Y}\widehat{Y}}=\widehat{\boldsymbol{S}}_{\widehat{Y}\widehat{Y}}-\widehat{P}+2\mu\frac{\partial\widehat{V}}{\partial\widehat{Y}}. \tag{1.27}$$

1.8 Solution method

Many phenomena in engineering and technology are nonlinear in nature and can be effectively represented using ordinary or partial differential equations. Finding the answer to these DEs is a difficult task due to the presence of strong nonlinearity. However, a variety of analytical and numerical techniques can be used to solve these equations. The following sections explain the fundamental concepts of a few different methods for solving (ODE) and (PDE).

i. Perturbation Technique

The perturbation technique is the most adaptable nonlinear dynamical model procedure, and it is constantly evolving and being used on increasingly complex problems. The perturbation method is based on the presence of perturbation quantities, which are small/large variables or parameters that can be found naturally in equations or artificially introduced for convenience. To put it another way, perturbation quantities are used to convert a nonlinear problem into many linear sub-problems. The addition of the solutions to the first few sub-problems, usually no more than two terms, is the solution to the problem.

Example

Consider a nonlinear DE

$$\frac{dg}{dt} + g = \varepsilon g^2 \tag{1.28}$$

with (IC's)

$$g(0) = 1. \tag{1.29}$$

By performing straight forward expansion around ε as in Eq. (1.28), we assume the solution.

$$g(\mathrm{t},\varepsilon) = g_0(\mathrm{t},\varepsilon) + \varepsilon g_1(\mathrm{t},\varepsilon) + ..., \tag{1.30}$$

placing the Eq. (1.30) in Eq. (1.29) and (1.28) we get

$$\frac{dg_0}{dt} + \varepsilon \frac{dg_1}{dt} + ... + (g_0 + \varepsilon g_1 + ...) = \varepsilon (g_0 + \varepsilon g_1 + ...)^2 \tag{1.31}$$

And

$$g_0(0)+\varepsilon g_1(0)+.....=1. \tag{1.32}$$

One can obtain the following systems by joining like powers of ε in Eqs. (1.31) and (1.32).

0^{th}- order system:

$$\frac{dg_0}{dt}+g_0=0, \qquad g_0(0)=1, \tag{1.33}$$

1^{st} -order system:

$$\frac{dg_1}{dt}+g_1=g_0{}^2, \qquad g_1(0)=0,\ g_1(0)=0 \tag{1.34}$$

Eqs. (1.33) and (1.34) have the following solutions:

$$g_0=e^{-t}, \tag{1.35}$$

$$g_1=e^{-t}-e^{-2t}, \tag{1.36}$$

Using Eqs. (1.35) –(1.36) in (1.30), we obtain

$$g(\mathrm{t},\varepsilon)=e^{-t}+\varepsilon\left(e^{-t}-e^{-2t}\right)+.....$$

CHAPTER 2

LITERATURE REVIEW

2.1 Overview

In this chapter, we have represented the study related to peristaltic transport of JS fluid in a tapered asymmetric channel, theory of lubrication approximation and MHD with viscous dissipation and thermal radiation.

2.2 Literature Review

Peristalsis is a pattern of fluid thrusting in ducts in which a progressive wave of area contraction or expansion propagates throughout the length of a fluid-filled distensible tube. Pumping fluid against an increase in pressure produces broad propulsive and mixing motions. Peristalsis is a biologically necessary component of smooth muscle contraction. It is a useful and automated system that controls numerous processes, including the movement of ovaries in the fallopian tube and the flow of bile from the gallbladder into the duodenum and bile from the kidney to the bladder. The peristalsis procedure can be applied to a variety of biological systems, such as the gastrointestinal tract's chyme movement, small blood vessels' blood flow, and the male reproductive system's duct afferents. Peristaltic pumping is also employed in industry for a few useful purposes, including the movement of hygienic fluids, the blood pump in heart-lung machines, and the movement of internal and hazardous fluids to prevent inclusion in the environment. Peristaltic phenomena are characterized as having important industrial uses in the strategy of roller pumps, which are used to pump fluids without being damaged by the connection with the pumping equipment. A positive displacement pump that is used to pump a variety of fluids is referred to as a peristaltic pump (often called a roller pump). There have been a lot of investigations into the peristaltic activity of liquids in a variety of physical contexts and flow geometries. Latham [1] examined the sinusoidal wall movement of viscous liquid. Shapiro et al. [2] employed lubrication theory to present a precise

summary of viscid fluid in peristaltic transport along a duct and tube. Abdelsalam et al. [3] examined the effects of various peristaltic factors while analyzing plasma flow with sinusoidal wall activity via a very small flexible artery using the lubrication hypothesis. Jeffrey liquid flowing with Newtonian fluid following peristaltic motion under the premise of minimal inertial forces and a small wave number was investigated by Kavitha et al. [4] The thermal radiative properties of a viscous liquid travelling over a porous surface are examined by Hussain et al. [5]. Theoretical simulations of magnetized Prandtl fluid flowing through a porous annulus are deliberated by Bhatti et al. [6]. Vaidya et al. [7] used the Rabinowitsch model with fluctuating liquid parameters to examine the sinusoidal wall explanation under the lubrication theory. The consequences of hydromagnetic peristaltic flow of Williamson liquid in a curved channel were investigated by Rashid et al. [8]. Rabinowitsch model with two compliant walls that obey peristalsis and the influence of variable liquid characteristics examined by Rajashekhar et al. [9]. The heat source and sink properties of the peristaltic transport of Prandtl-Eyring nanomaterial over the channel boundaries were studied by Akram et al. [10]. They showed that raising the parameters for wall mass and tension enhances liquid velocity, while increasing the value for wall damping has the opposite effect. The theory of lubrication approximation was implemented by Abbas et al. [11] to explain the effect of the activation energy research on the peristalsis of Casson fluid in a non-uniform tube under the effects of thermal radiation. [12–15] contains more works that are pertinent to this topic.

Theoretical modelling of NNF is crucial for predicting and comprehending the behavior of a wide range of emergent natural processes. Many natural fluids, including plasma, fuel, lubricants, oils, clay, and polymer solutions, have substantial rheologic assets which do not follow the Newton's law of viscosity's usual direct relationship between strain and stress. The performance of NNF in modern industries and technology may generate a lot of interest in the issue (see refs. [16–17]). On the other hand, the constitutive terms which are involved in modelling such fluids are often complex, making obtaining exact solutions challenging. This study took the Jonhson-Segalman fluid into account. Johnson-Segalman liquid is one of the NNF imperative subclass that can describe the "spurt" fact [18]. The term "spurt" has been used to designate a huge rise in

volume with a minor upsurge in intensity in a driving rate of pressure. In a driving pressure gradient, the term "spurt" has been used to represent a high rise in volume with a little increase in intensity. Investigation of the peristaltic transport of Johnson-Segalman liquid in a curved geometry using lubrication theory to simplify the normalized equations is discussed by Hina et al. [19]. Kothandapani et al. [20] performed a theoretical examination of the peristaltic activity of Johnson-Segalman material within a microfluidic tapered pipe and determined that when the non-uniform factor is increased, pressure rise is more influenced in the free pumping area. A few more explorations into different geometries can be found in the references [21–22].

Numerous researchers are interested in the study of magnetohydrodynamic (MHD) peristaltic motion due to its expanding applications in areas such as plasma pumping, producing, medication targeting, (MRI), magnetotherapy, hyperthermia, and others. The hydromagnetic Williamson fluid's oscillatory propagation was bent by Rashid et al. [23]. Akram et al. [24] used the lubrication theory to evaluate the diffusion of Prandtl nanomaterials in the presence of Lorentz force along a non-uniform conduit with sinusoidal walls. Abbas et al. [25] reported and obtained analytical conclusions concerning the impact of Lorentz force in a channel on the peristalsis phenomenon of Jeffrey liquid. They noticed that increasing the Brinkman number caused a rise in the thermal profile. The importance of entropy analysis for the movement of hydromagnetic, viscid liquid peristalsis in a changing tube using lubrication theory approximation was recently investigated by Abbas et al. [26]. Some recent demonstrative inquiries in this approach might be found at [27–29]. Additionally, thermal radiation effects are significant on heat transfer in industry, particularly in the design of gas turbines, nuclear power plants, missiles, spacecraft, satellites, and other manufacturing and industrial machinery. It has been proven that thermal radiation works well in a variety of extreme-temperature processes. Nisar et al. [30] examined the radiative properties of the peristaltic interest of Eyring-Powell nanomaterial in flexible channel walls. The main conclusion of this study is that raising the thermal Biot number lowers the radiative profile while raising it for parameters affecting Brownian flow and thermophoresis. The thermal study of the peristaltic activity of Rabinowitch fluid in a channel was examined by Imran et al. [31]. Alsaedi et al. [32] also investigated how hall current affected the sinusoidal wall transport

of oily nanomaterials along a conduit. [33–36] contains more analyses of heat conduction by thermal radiation. Non-pregnant myometrial contractions can occur in both symmetrical and asymmetrical directions, which results in a peristaltic-type liquid transfer uterus problem known as intrauterine liquid transport. In addition, it is investigated that the intrauterine carriage of fluid in a uterus at the sagittal cross over reveals a narrow channel surrounded by two relatively comparable walls as well as wave trains with different time differences and scales [37–39]. Aside from the research indicated above, we are particularly interested in investigating the effect of heat transport phenomena on the peristaltic movement of an electrically conducting Johnson-Segalman liquid in a tapered channel with velocity slip circumstances. It is worth mentioning that such a study does not appear to be available in the current literature. The formulas governing the flow of the Johnson-Segalman liquid are simplified by lubrication theory. The perturbation technique is used to derive the following equations, and the physical properties of key variable quantities are investigated and explained using graphs.

CHAPTER 3

A TAPERED ASYMMETRIC CHANNEL WITH NONLINEAR PERISTALTIC MOTION OF JOHNSON-SEGALMAN FLUID

3.1 Overview

This comparative study discusses the nonlinear peristaltic transport of Johnson-Segalman fluid in a thin asymmetric channel. The thin asymmetric channel was formed as a peristaltic wave train passed by beyond non-uniform walls with unique amplitudes and phases. Assumptions of low Reynolds number and long wavelength were used to simplify the Johnson-Segalman fluid's 2-D equations. In order to solve the streamline, pressure gradient, and axial velocity equations, the regular perturbation method is used.

3.2 Mathematical formulation

Consider (2-D) channel that is infinitely asymmetric and contains an incompressible Johnson-Segalman fluid. The coordinate approach employed is rectangular, with X horizontal to the channel walls and Y perpendicular to them. There is also a proposal for an immense wave train travelling at c alongside the channel walls. The peristaltic wave train on the walls exhibits irregular amplitudes and phases. The channel walls have a specific shape.

$$H_2\left(\widehat{X},t'\right)=a_2\sin\left(\frac{2\pi\widehat{X}}{\lambda}-\frac{ct'}{\lambda}\right)+d+k'\widehat{X}, \tag{3.1}$$

$$H_1\left(\widehat{X},t'\right)=-a_1\sin\left(\frac{2\pi\widehat{X}}{\lambda}-\frac{ct'}{\lambda}+\phi\right)-d-k'\widehat{X}, \tag{3.2}$$

where $\phi \in [0, \pi]$ the difference of phases and the waves amplitudes are a_1 and a_2. Waves in phase are designated by $\phi = \pi$,while waves out of phase are designated by $\phi = 0$ Furthermore d_1, d_2, a_1, a_2 and ϕ satisfy the condition.

$$a_1^2 + a_2^2 + 2a_1 a_2 cos\phi \leq (2d)^2 . \tag{3.3}$$

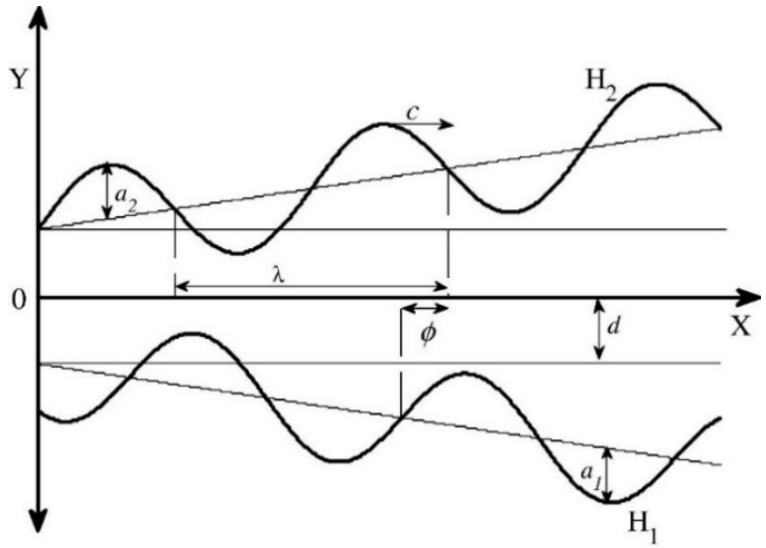

Figure 3.1: Problems geometry

An incompressible fluid flow equations are as follows:[18]

$$div\boldsymbol{V} = 0, div\boldsymbol{\tau} = \rho \frac{\partial \boldsymbol{V}}{\partial t}, \tag{3.4}$$

For a (JS) fluid, the Cauchy stress tensor is defined in Chapter one using Eqs. (1.16) - (1.18). For e=1, model (3.4) is reduced to the Maxwell fluid model, which is then recovered as the traditional NS fluid model by taking $\mu = 0$. In the context of the situation, the 2-D flow velocity is depicted.

$$\boldsymbol{V} = \left[\widehat{U}\left(\widehat{X}, \widehat{Y}, t'\right), \widehat{V}\left(\widehat{X}, \widehat{Y}, t'\right), 0\right], \tag{3.5}$$

From Eqs. (3.4) and (1.16) - (1.18), we have

$$\frac{\partial \widehat{U}}{\partial \widehat{X}}+\frac{\partial \widehat{V}}{\partial \widehat{Y}}=0, \tag{3.6}$$

$$\rho\left(\frac{\partial}{dt^{'}}+\widehat{U}\frac{\partial}{\partial \widehat{X}}+\widehat{V}\frac{\partial}{d\widehat{Y}}\right)\widehat{U}=\frac{\partial \widehat{S}_{\widehat{X}\widehat{X}}}{\partial \widehat{X}}+\frac{\partial \widehat{S}_{\widehat{X}\widehat{Y}}}{\partial \widehat{Y}}-\frac{\partial \widehat{P}}{\partial \widehat{X}}+\mu\left(\frac{\partial^2}{\partial \widehat{X}^2}+\frac{\partial^2}{\partial \widehat{Y}^2}\right)\widehat{U}, \tag{3.7}$$

$$\rho\left(\frac{\partial}{dt^{'}}+\widehat{U}\frac{\partial}{\partial \widehat{X}}+\widehat{V}\frac{\partial}{d\widehat{Y}}\right)\widehat{V}=\frac{\partial \widehat{S}_{\widehat{Y}\widehat{Y}}}{\partial \widehat{X}}+\frac{\partial \widehat{S}_{\widehat{X}\widehat{Y}}}{\partial \widehat{Y}}-\frac{\partial \widehat{P}}{\partial \widehat{Y}}+\mu\left(\frac{\partial^2}{\partial \widehat{X}^2}+\frac{\partial^2}{\partial \widehat{Y}^2}\right)\widehat{V}, \tag{3.8}$$

$$2\eta\frac{\partial \widehat{U}}{\partial \widehat{X}}=\widehat{S}_{\widehat{X}\widehat{X}}-2em\widehat{S}_{\widehat{X}\widehat{X}}\frac{\partial \widehat{U}}{\partial \widehat{X}}+m\widehat{S}_{\widehat{X}\widehat{X}}\left[\frac{\partial}{dt^{'}}+\widehat{U}\frac{\partial}{\partial \widehat{X}}+\widehat{V}\frac{\partial}{d\widehat{Y}}\right]$$
$$+m\widehat{S}_{\widehat{X}\widehat{Y}}\left[(1-e)\frac{\partial \widehat{V}}{\partial \widehat{X}}-(1+e)\frac{\partial \widehat{U}}{\partial \widehat{Y}}\right], \tag{3.9}$$

$$\left(\eta\frac{\partial \widehat{U}}{\partial \widehat{Y}}+\eta\frac{\partial \widehat{V}}{\partial \widehat{X}}\right)=\widehat{S}_{\widehat{X}\widehat{Y}}+m\widehat{S}_{\widehat{X}\widehat{Y}}\left[\frac{\partial}{dt^{'}}+\widehat{U}\frac{\partial}{\partial \widehat{X}}+\widehat{V}\frac{\partial}{d\widehat{Y}}\right]+\frac{m}{2}\widehat{S}_{\widehat{X}\widehat{X}}\left[(1-e)\frac{\partial \widehat{U}}{\partial \widehat{Y}}-(1+e)\frac{\partial \widehat{V}}{\partial \widehat{X}}\right]$$
$$+\frac{m}{2}\widehat{S}_{\widehat{Y}\widehat{Y}}\left[(1-e)\frac{\partial \widehat{V}}{\partial \widehat{X}}-(1+e)\frac{\partial \widehat{U}}{\partial \widehat{Y}}\right], \tag{3.10}$$

$$2\eta\frac{\partial \widehat{V}}{\partial \widehat{Y}}=\widehat{S}_{\widehat{Y}\widehat{Y}}-2em\widehat{S}_{\widehat{Y}\widehat{Y}}\frac{\partial \widehat{V}}{\partial \widehat{Y}}+m\widehat{S}_{\widehat{Y}\widehat{Y}}\left[\frac{\partial}{dt^{'}}+\widehat{U}\frac{\partial}{\partial \widehat{X}}+\widehat{V}\frac{\partial}{d\widehat{Y}}\right]$$
$$+m\widehat{S}_{\widehat{X}\widehat{Y}}\left[(1-e)\frac{\partial \widehat{U}}{\partial \widehat{Y}}-(1-e)\frac{\partial \widehat{V}}{\partial \widehat{X}}\right], \tag{3.11}$$

Defining dimensionless quantities

$$x=\frac{\widehat{X}}{\lambda}, y=\frac{\widehat{Y}}{d}, t=\frac{ct^{'}}{\lambda}, u=\frac{\widehat{U}}{c}, v=\frac{\widehat{V}}{c}, \delta=\frac{d}{\lambda}, h_1=\frac{H_1}{d}, h_2=\frac{H_2}{d}\ \ p=\frac{d^2\widehat{P}}{c\lambda\mu}, s_{ij}=\frac{d}{\mu c}\widehat{S_{ij}}\left(\widehat{X}\right),$$

$$Re=\frac{\rho cd}{\mu}, We=\frac{mc}{d},\ a=\frac{a_1}{d},\ b=\frac{a_2}{d}\ \ p=\frac{d^2}{\lambda(\mu+\eta)c}\widehat{P}\left(\widehat{X}\right), k=\frac{\lambda k^{'}}{d}. \tag{3.12}$$

Using (3.12) into the Eqs. (3.6) - (3.11) with the help of $u=\psi_y, v=-\delta\psi_x$ we have

$$Re\delta\left(\psi_y\psi_{xy}-\psi_x\psi_{yy}\right)=-\frac{\partial p}{\partial x}\left(\frac{\mu+\eta}{\mu}\right)+\delta\frac{\partial}{\partial x}\left(s_{xx}\right)+\frac{\partial}{\partial y}\left(s_{xy}\right)+\left(\delta^2\psi_{xxy}+\psi_{yyy}\right), \tag{3.13}$$

$$-Re\delta^3\left(\psi_y\psi_{xx}-\psi_x\psi_{xy}\right)=-\frac{\partial p}{\partial y}\left(\frac{\mu+\eta}{\mu}\right)+\delta^2\frac{\partial}{\partial x}\left(s_{yx}\right)+\delta\frac{\partial}{\partial y}\left(s_{yy}\right)-\delta^2\begin{pmatrix}\delta^2\psi_{xxx}\\+\psi_{xyy}\end{pmatrix}, \tag{3.14}$$

$$\left(\frac{2\eta\delta}{\mu}\right)\psi_{xy}=s_{xx}-2emWe\delta\psi_{xy}+We\delta\left[\psi_y\frac{\partial}{\partial x}\left(s_{xx}\right)-\psi_x\frac{\partial}{\partial y}\left(s_{xx}\right)\right]$$
$$-Wes_{xy}\left[\delta^2\left(1-e\right)\psi_{xx}+\left(1+e\right)\psi_{yy}\right], \tag{3.15}$$

$$\frac{\eta}{\mu}\left(\psi_{yy}-\delta^2\psi_{xx}\right)=s_{xy}+We\left[\psi_y\frac{\partial}{\partial x}(s_{xy})-\psi_x\frac{\partial}{\partial y}(s_{xy})\right]$$
$$+\frac{We}{2}s_{xx}\left[(1-e)\psi_{yy}+\delta^2(1+e)\psi_{xx}\right]-\frac{We}{2}s_{yy}\left[\delta^2(1-e)\psi_{xx}+(1+e)\psi_{yy}\right], \tag{3.16}$$

$$-\left(\frac{2\eta\delta}{\mu}\right)\psi_{xy}=s_{xy}+We\delta\left[\psi_y\frac{\partial}{\partial x}(s_{yy})-\psi_x\frac{\partial}{\partial y}(s_{yy})\right]$$
$$+2eWe\delta s_{yy}\psi_{xy}+Wes_{xy}\left[(1-e)\psi_{yy}+(1+e)\delta^2\psi_{xx}\right], \tag{3.17}$$

Using the approximation theory of lubrication ($\mathrm{Re}\to 0$ and $\delta << 1$), Equations (3.13)-(3.17) develops as follows:

$$\frac{\partial}{\partial y}s_{xy}+\psi_{yyy}=\left(\frac{\mu+\eta}{\mu}\right)\frac{\partial p}{\partial x}, \tag{3.18}$$

$$\frac{\partial p}{\partial y}=0, \tag{3.19}$$

$$s_{xx}=We\left(1+e\right)\psi_{yy}s_{xy}, \tag{3.20}$$

$$\frac{\eta}{\mu}\psi_{yy}=s_{xy}+\frac{We}{2}\left(1-e\right)\psi_{yy}s_{xx}-\frac{We}{2}\left(1+e\right)\psi_{yy}s_{yy}, \tag{3.21}$$

$$s_{yy}=-We\left(1-e\right)\psi_{yy}s_{xy}, \tag{3.22}$$

Eq (3.19) also suggests that with this approximation. $p\neq p(y)$. Removal of ψ after Eqs. (3.18) and (3.19) generates

$$\frac{\partial^2}{\partial y^2}s_{xy}+\psi_{yyyy}=0, \tag{3.23}$$

Using Eqs. (3.20) and (3.22) into Eqs. (3.21), we have

$$s_{xy} = \frac{\left(\frac{\eta}{\mu}\right)\psi_{yy}}{1+We^2\left(1-e^2\right)\left(\psi_{yy}\right)^2}, \tag{3.24}$$

Using Eq. (3.24) in Eqs. (3.18) and (3.23), We can write

$$\frac{\partial^2}{\partial y^2}\left[\frac{\left(\frac{\eta}{\mu}+1\right)\psi_{yy}+We^2\left(1-e^2\right)\left(\psi_{yy}\right)^3}{1+We^2(1-e^2)\left(\psi_{yy}\right)^2}\right]=0, \tag{3.25}$$

$$\left(\frac{\mu+\eta}{\mu}\right)\frac{\partial p}{\partial x}=\psi_{yyy}+\frac{\partial}{\partial y}\left[\frac{(\frac{\eta}{\mu})\psi_{yy}}{1+We^2\left(1-e^2\right)\left(\psi_{yy}\right)^2}\right]=0, \tag{3.26}$$

The following are the problem's relevant boundary conditions:

$$\begin{aligned} &\psi=\frac{F}{2}, \quad \frac{\partial\psi}{\partial y}=0, \quad && at\ y=h_2, \\ &\psi=-\frac{F}{2}, \quad \frac{\partial\psi}{\partial y}=0, \quad && at\ y=h_1. \end{aligned} \tag{3.27}$$

3.3 Solution of the problem

When using binomial for small We^2, Eqs. (3.25) and (3.26), may be simplified

$$\frac{\partial^2}{\partial y^2}\left[\psi_{yy}+We^2\alpha_1(\psi_{yy})^3+We^4\alpha_2(\psi_{yy})^5\right]=0, \tag{3.28}$$

$$\frac{\partial p}{\partial x}=\psi_{yyy}+We^2\alpha_1\frac{\partial}{\partial y}\left[(\psi_{yy})^3\right]+We^4\alpha_2\frac{\partial}{\partial y}\left[(\psi_{yy})^5\right], \tag{3.29}$$

where, $\alpha_1=\frac{(e^2-1)\eta}{(\eta+\mu)}, \alpha_2=(e^2-1)\alpha_1,$

0^{th} - order system

$$\frac{\partial^4 \psi_0}{\partial y^4} = 0, \tag{3.30}$$

$$\frac{\partial p_0}{\partial x} = \frac{\partial^3 \psi_0}{\partial y^3}, \tag{3.31}$$

$$\begin{aligned} &\psi_0 = \frac{F}{2}, \quad \frac{\partial \psi_0}{\partial y} = 0, && at\ y = h_2, \\ &\psi_0 = -\frac{F}{2}, \quad \frac{\partial \psi_0}{\partial y} = 0, && at\ y = h_1. \end{aligned} \tag{3.32}$$

1^{st} - order system

$$\frac{\partial^4 \psi_1}{\partial y^4} = -\alpha_1 \frac{\partial^2}{\partial y^2}\left[\left(\frac{\partial^2 \psi_0}{\partial y^2}\right)^3\right], \tag{3.33}$$

$$\frac{\partial p_1}{\partial x} = \frac{\partial}{\partial y}\left[\frac{\partial^2 \psi_1}{\partial y^2} + \alpha_1\left(\frac{\partial^2 \psi_0}{\partial y^2}\right)^3\right], \tag{3.34}$$

$$\begin{aligned} &\psi_1 = \frac{F}{2}, \quad \frac{\partial \psi_1}{\partial y} = 0, && at\ y = h_2, \\ &\psi_1 = -\frac{F}{2}, \quad \frac{\partial \psi_1}{\partial y} = 0, && at\ y = h_1. \end{aligned} \tag{3.35}$$

2^{nd} - order system

$$\frac{\partial^4 \psi_2}{\partial y^4} = -3\alpha_1 \frac{\partial^2}{\partial y^2}\left[\frac{\partial^2 \psi_1}{\partial y^2}\left(\frac{\partial^2 \psi_0}{\partial y^2}\right)^2\right] - \alpha_2 \frac{\partial^2}{\partial y^2}\left[\left(\frac{\partial^2 \psi_0}{\partial y^2}\right)^5\right], \tag{3.36}$$

$$\frac{\partial p_2}{\partial x} = \frac{\partial^3 \psi_2}{\partial y^2} + 3\alpha_1 \frac{\partial}{\partial y}\left[\frac{\partial^2 \psi_1}{\partial y^2}\left(\frac{\partial^2 \psi_0}{\partial y^2}\right)^2\right] + \alpha_2 \frac{\partial}{\partial y}\left[\left(\frac{\partial^2 \psi_0}{\partial y^2}\right)^5\right], \tag{3.37}$$

$$\begin{aligned} &\psi_2 = \frac{F}{2}, \quad \frac{\partial \psi_2}{\partial y} = 0, && at\ y = h_2, \\ &\psi_2 = -\frac{F}{2}, \quad \frac{\partial \psi_2}{\partial y} = 0, && at\ y = h_1. \end{aligned} \tag{3.38}$$

Solving the above systems yields axial velocity, stream function, and pressure gradient.

The usual increase in Δp concluded one wavelength period is given by

$$\Delta p = \int_0^1 \int_0^1 \frac{\partial p}{\partial x} dx dt. \tag{3.39}$$

3.4 Graphical results and discussion

We consider that the instantaneous volume rate $F(x,t)$ of flow is periodic in $(x-t)$ to examine the quantitative results obtained.

$$\mathrm{F}(x,t) = Q + \mathrm{a}\sin 2\pi(\mathrm{x}-\mathrm{t}) + \mathrm{b}\sin[2\pi(\mathrm{x}-\mathrm{t}) + \phi]. \tag{3.40}$$

Q is the flow's average time value throughout a single wave period.

The integration of $\frac{\partial p}{\partial x}$ is used in the expression for Δp. Eq. (3.39) is not integrable analytically due to the complexity of $\frac{\partial p}{\partial x}$. As a result, the evaluation of the integrals necessitates the use of a numerical integration scheme. The result is executed with the help of MATHEMATICA, and all graphs were made for several values of the variables of importance. Because the (PDE) system resulting from the mathematical modelling of the problem at hand is strongly nonlinear and coupled, it cannot be used directly for the analytical solution. As a result, the formulas for axial velocity, pressure rise, and streamlines are handled and checked for differences in flow parameters. Figures (3.2 - 3.7) exhibits a graph of the Δp vs. the change in time-average flux Q . Figures. (3.2 - 3.7) demonstrate pumping zones such as peristaltic injecting $(\mathrm{Q} > 0, \Delta\,\mathrm{p} > 0)$ enhanced driving $(\mathrm{Q} > 0, \Delta\,\mathrm{p} < 0)$, and backward injecting $(\mathrm{Q} < 0, \Delta\,\mathrm{p} > 0)$). Figure 3.2 depicts the Δp as a function of (a) . As shown in Fig. 3.3, the peristaltic pumping section and free thrusting $(\Delta\,\mathrm{p} = 0)$ diminish as the non-consistent factor (k) increases, and the situation is remarkably like that of enhanced pumping. For various values of (We), Figure 3.4 depicts the variance of Δp vs Q . The pumping rate drops as (We) increases, and the free pumping bends seem to be intersecting. The graph in Figure 3.5 shows that the Q rises as Δp diminishes, and the pumping area shrinks as the amplitude of phase difference

(ϕ) rises. For several values of the slip factor (e), the plots of Δp against Q are shown in Fig. 3.6. It illustrates that the dispersal of Δp in a rising trend due to the slip factor (e) is nonlinear. The fluctuations of the dynamic viscosity factor on Δp against Q are shown in Figure 3.7. The Δp is reduced by enhancing the dynamic viscosity factor (η) in the enhanced pumping zone $(\Delta p < 0 \text{ and } Q > 0)$, as shown in this graph. The nonlinear nature of the curves depicting the Δp against Q is reflected in the nonlinear nature of the curves for large values of (η). Fig. 3.8 shows the impact of the bottom wall's amplitude (a) on the axial velocity. The axial velocity rises by rising (a). Figure 3.9 depicts the influence of the slip factor (e) on u. The axial velocity u seems to decline in the trapped asymmetric channel's nearer lower and upper halves; however, the differing comportment seems to be reflected in the trapped channel's core region. The velocity dispersal of the liquid is studied for several variations of the dynamic viscosity factor (η) non-uniform factor (k), and (We) in Figures (3.10 - 3.12). The graphs show that increasing the values of (η), (k), and (We) lowers the axial velocity in the tapered asymmetric channel's central area. The impact of Q on the u allocation is seen in Figure 3.13. It demonstrates that when Q rises, u rises with it.

Another interesting aspect of the occurrence is the trapping (PT). When closed streamlines in a reference wave structure form an internally moving bolus of fluid, the peristaltic wave pushes it forward. Bolus can also be discovered in the fixed frame, owing to the impact of a time-average of the stream over a single wave period which is nonzero. Figure 3.14 depicts the streamlines for various s values. It's also worth noting that when a increases, the amount of the bolus grows. The sound impacts of (We) on trapping are depicted in Fig.3.15 for the tapered asymmetric channel. The bolus is irregular around the centerline, as seen in Figure 3.15(a), and its size reduces as (We) rises. Figure 3.16 shows the effect of Q on the streamlines. The trapped bolus grows, and further trapped bolus seems as Q rises.

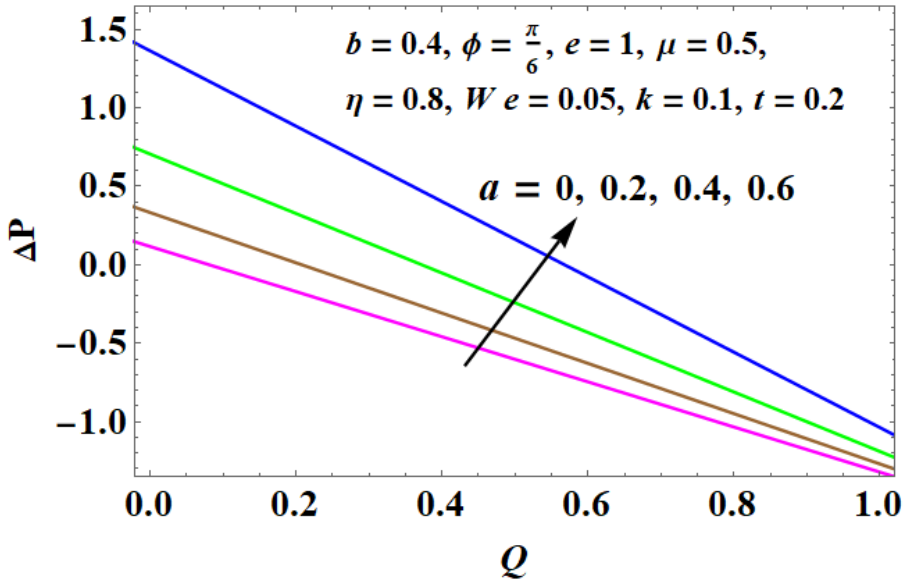

Figure 3.2: Upshot of a on pressure

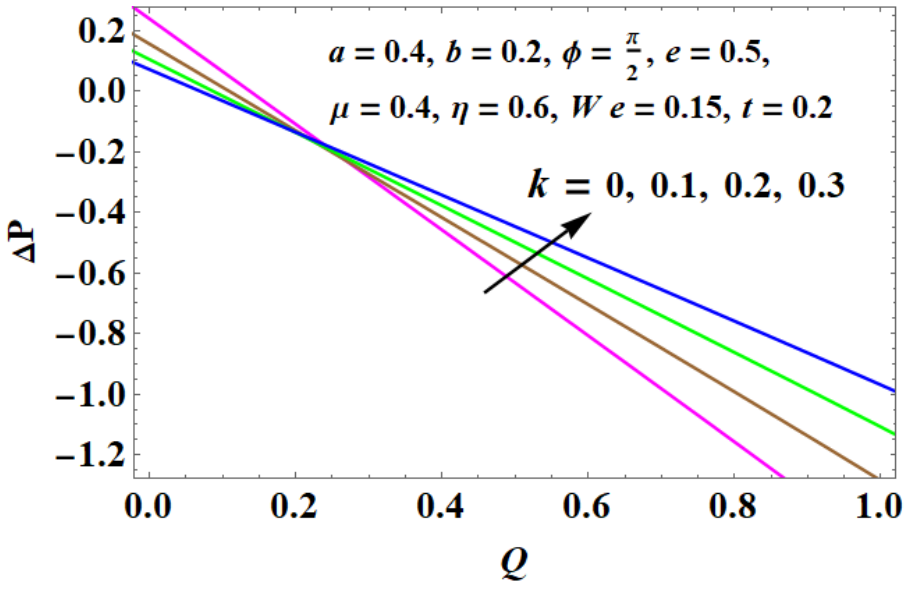

Figure 3.3: Upshot of k on pressure

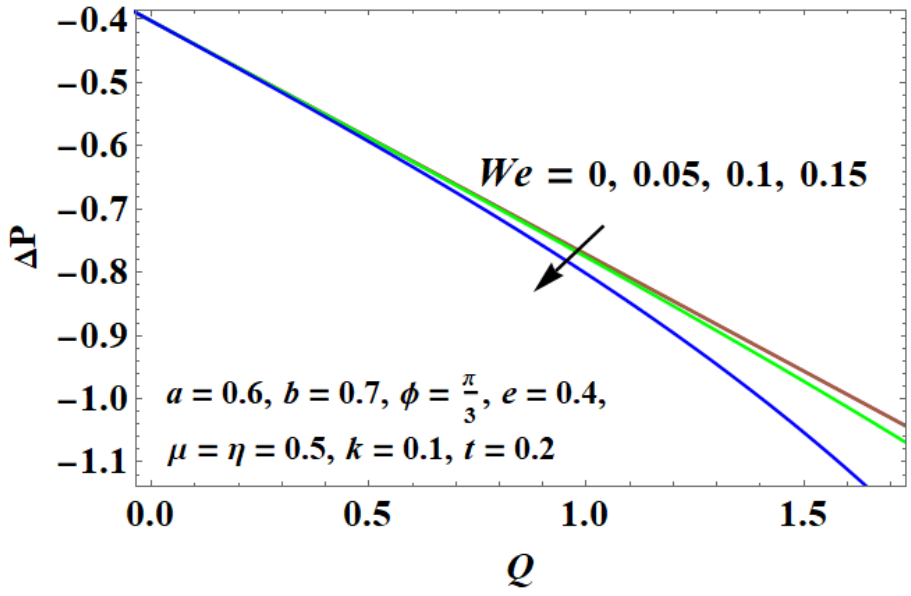

Figure 3.4: Upshot of We on pressure.

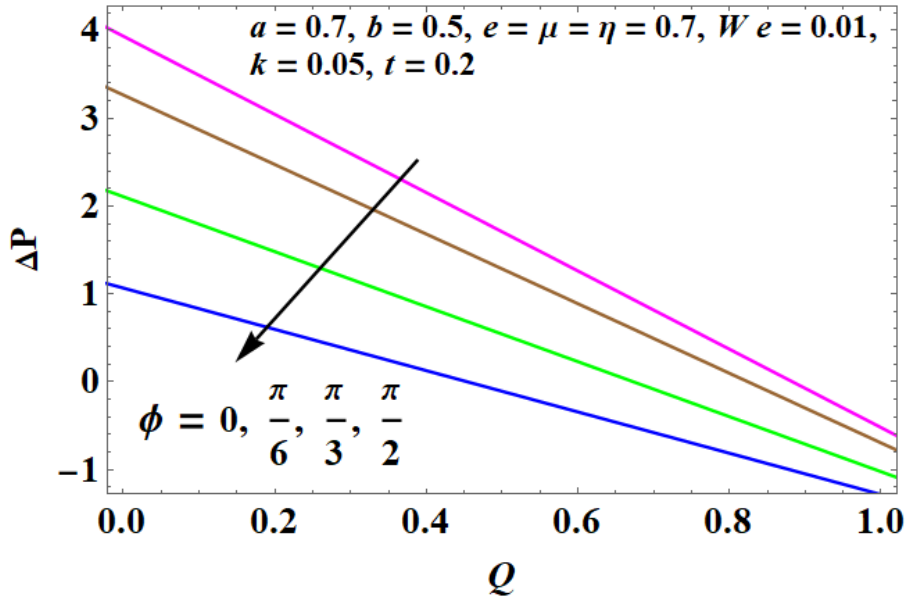

Figure 3.5: Upshot of ϕ on pressure.

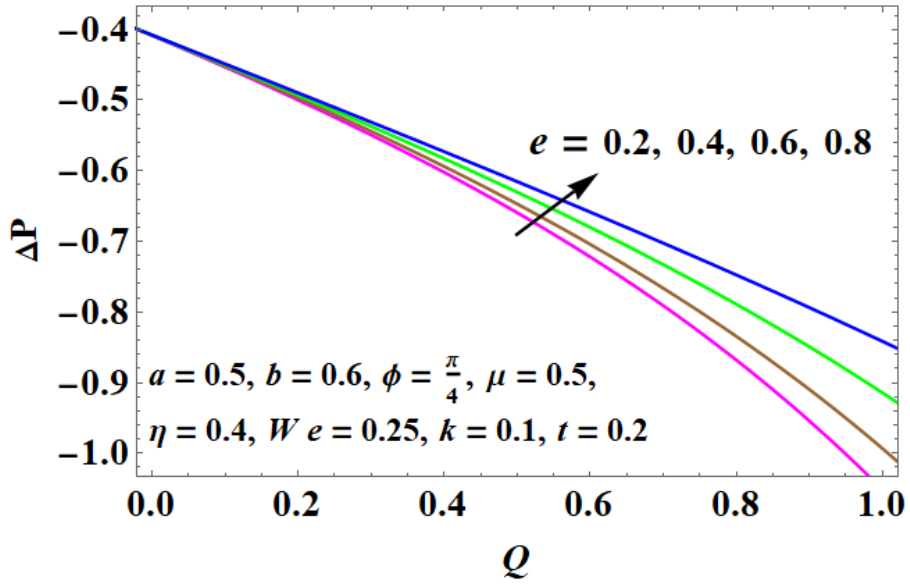

Figure 3.6: Upshot of e on pressure.

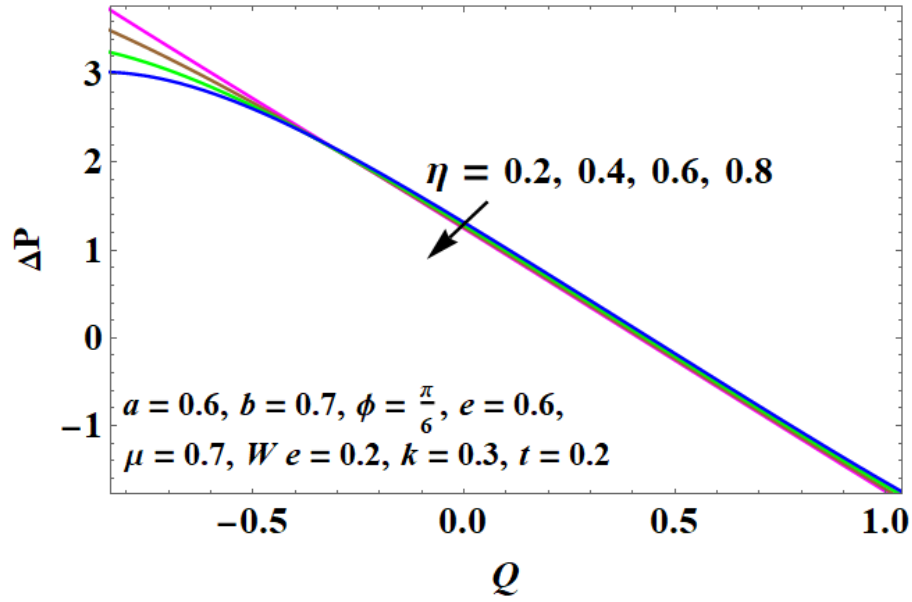

Figure 3.7: Upshot of η on pressure.

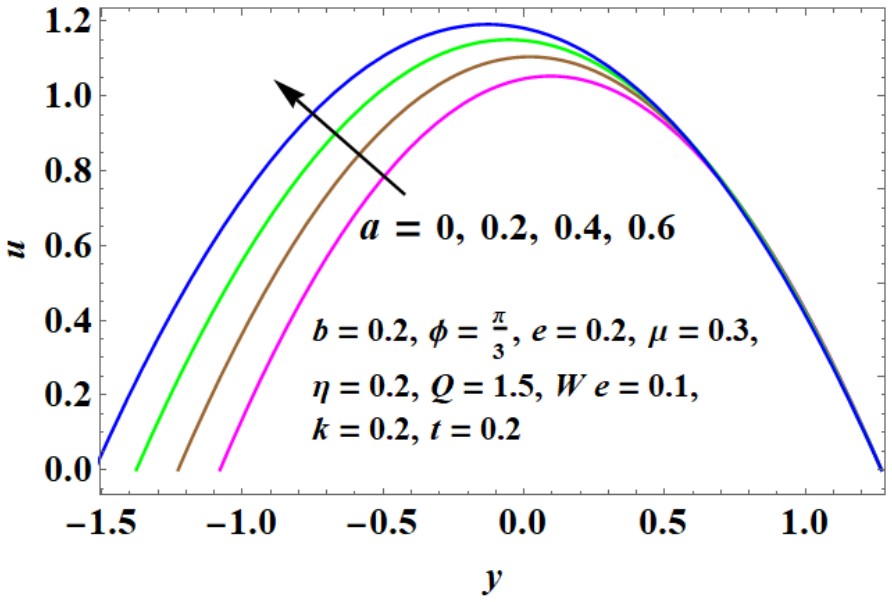

Figure 3.8: Upshot of a on axial velocity.

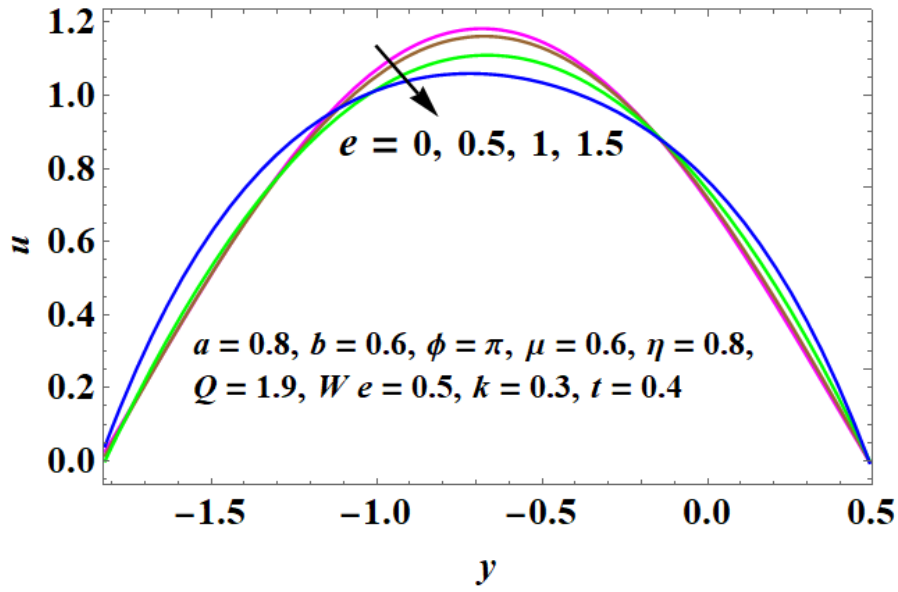

Figure 3.9: Upshot of e on axial velocity

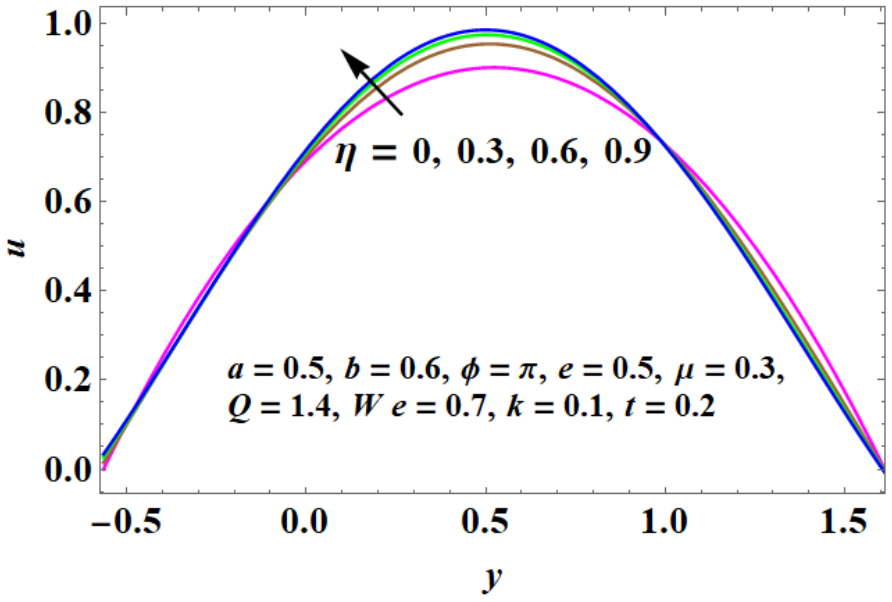

Figure 3.10: Upshot of η on axial velocity.

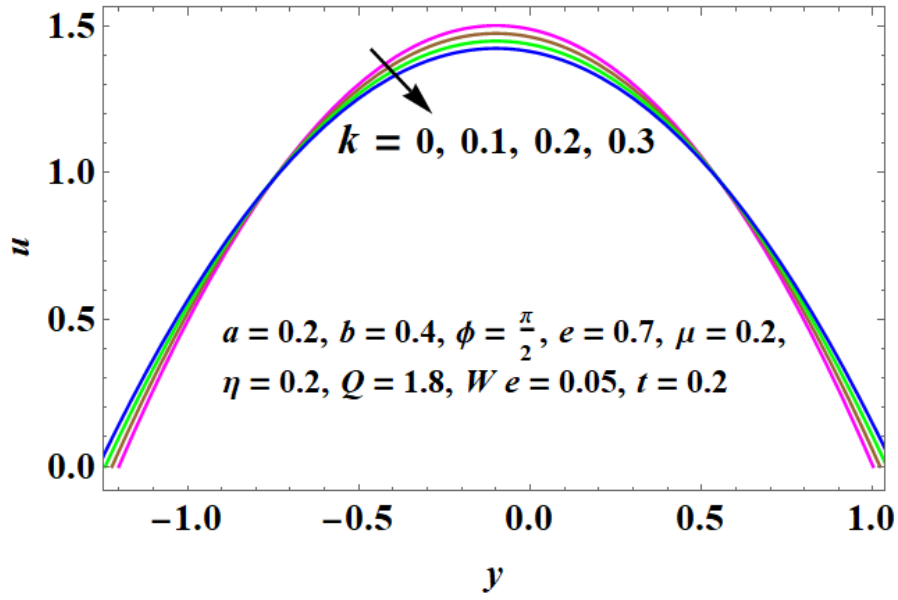

Figure 3.11: Upshot of k on axial velocity

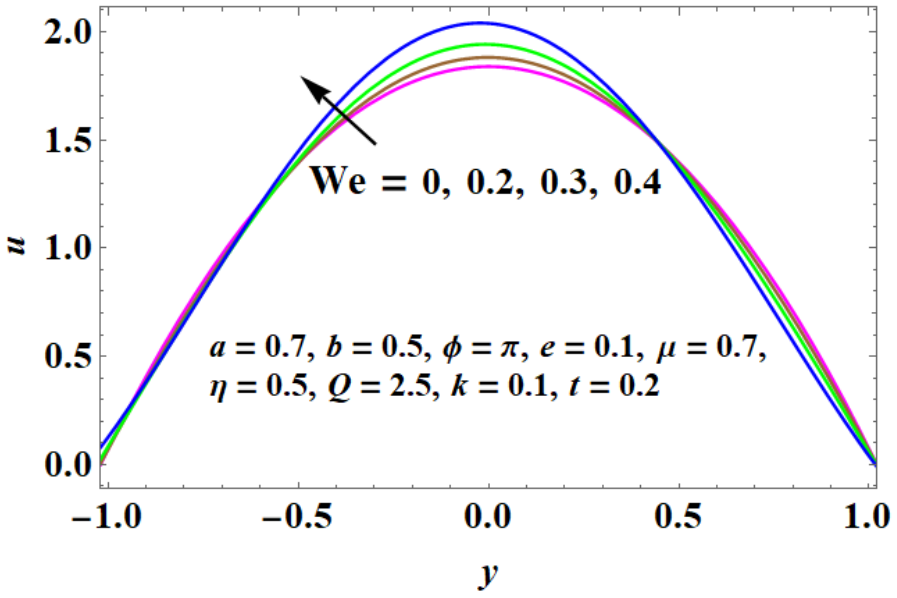

Figure 3.12: Upshot of We on axial velocity.

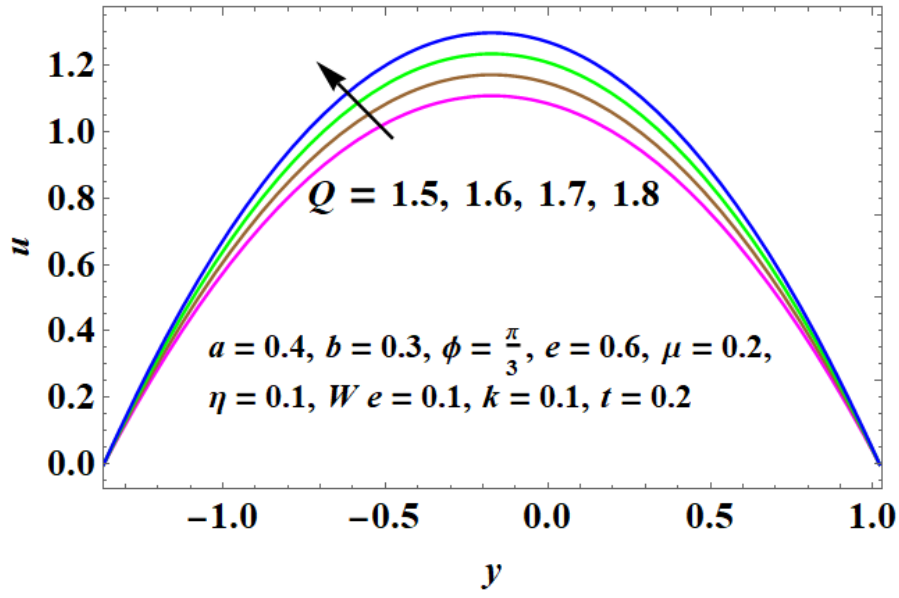

Figure 3.13: Upshot of Q on axial velocity

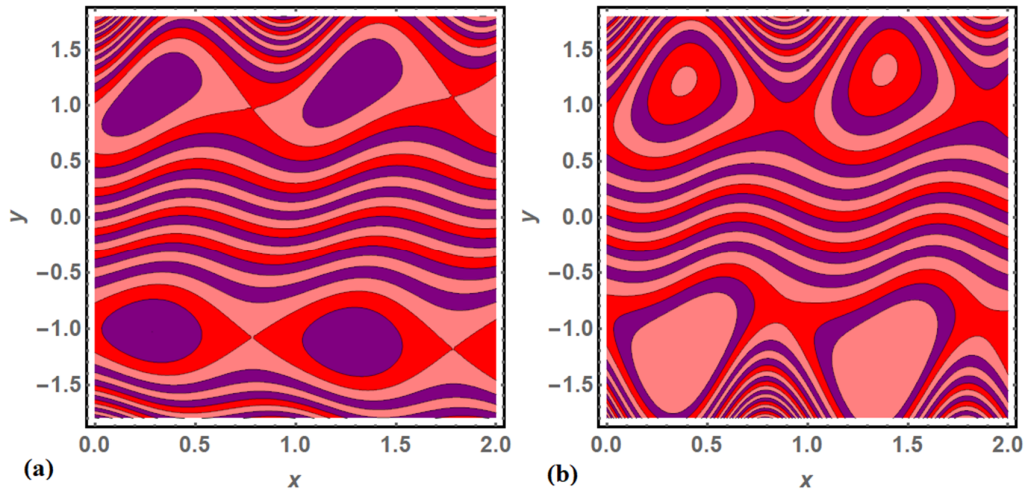

Figure 3.14: Streamlines for different values of (a) $a = 0$,(b) $a = 0.3$ while other factors are $b = 0.2,\ \phi = \frac{\pi}{3},\ e = 0.7,\ \mu = 0.8,\ \eta = 0.5,\ Q = 1.8,\ We = 0.1,\ k = 0.1,\ t = 0.2$

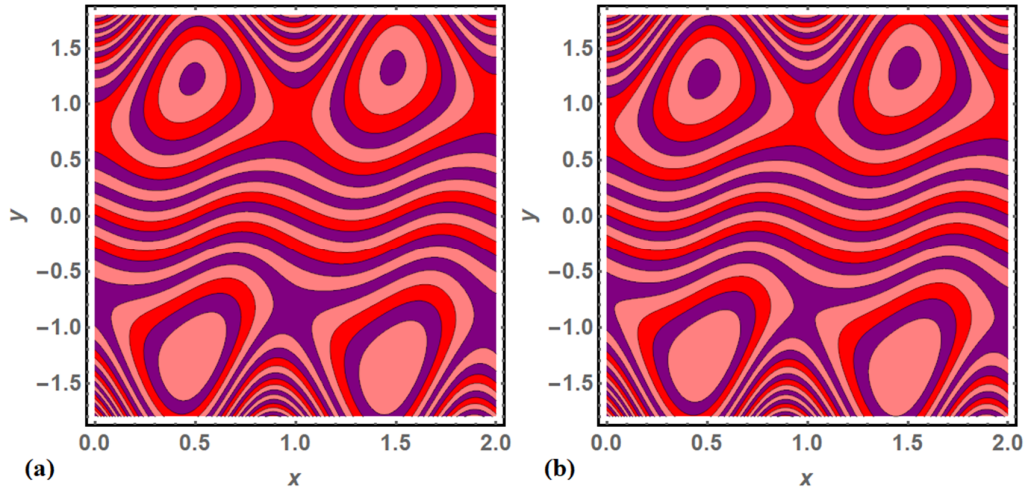

Figure 3.15: Streamlines for different values of (a) $Q = 1.5$,(b) $Q = 1.6$ while other factors are $a = 0.3,\ b = We = e = 0.2,\ \phi = \frac{\pi}{3},\ \mu = 0.8,\ \eta = 0.5,\ k = 0.1,\ t = 0.3$

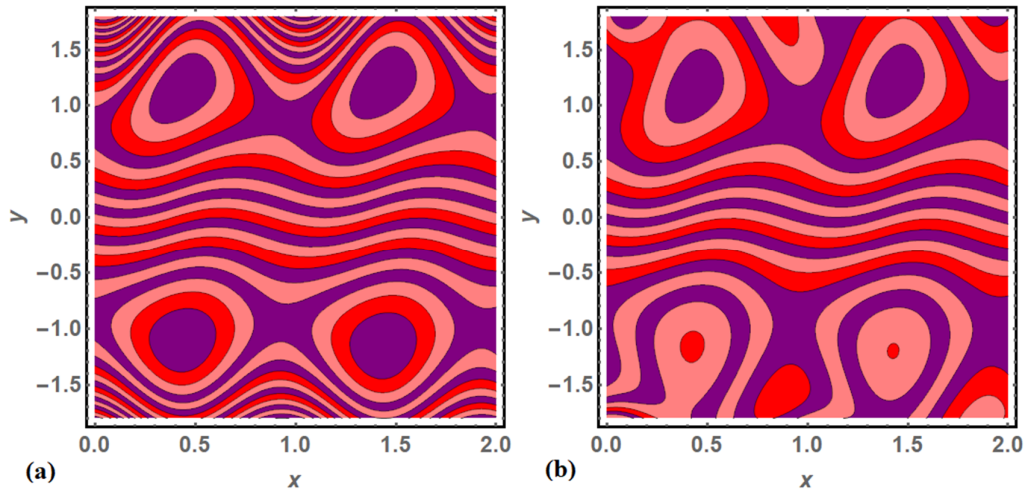

Figure 3.16: Streamlines for different values of (a) $We = 0$,(b) $We = 0.6$ while other factors are $a = 0.1,\ b = 0.2,\ \phi = \frac{\pi}{3},\ e = 0.4,\ \mu = 0.1,\ \eta = 0.8,\ Q = 1.2,\ k = 0.05,\ t = 0.3$.

CHAPTER 4

HEAT TRANSFER ANALYSIS OF JOHNSON-SEGALMAN FLUID IN TAPERED ASYMMETRIC CHANNEL

4.1 Overview

This chapter examines the heat transfer study of a Johnson-Segalman liquid in a tapered asymmetric channel, MHD with viscous dissipation and radiation effects. To create the Johnson-Segalman fluid model's governing equations, dimensionless variables were used. Using the perturbation approach, we can resolve these equations. At the conclusion, the results will be shown in graphs.

4.2 Problem Statement

Consider an incompressible peristaltic motion of electrically conducting Johnson-Segalman liquid through a two-dimensional tapering channel with velocity slip at upper and lowers walls. Flow inside the thin channel is produced by the trains of sinusoidal waves moving alongside the walls of the channel with constant speed c. We employ a rectangular coordinate system in such a manner that $X-$axis is taken in the flow direction and $Y-$axis is taken perpendicular to the direction of flow (see Fig. 4.1). A uniform applied magnetic field is employed in the oblique direction with strength $\boldsymbol{B}_0$. For the peristaltic pattern, the wave trains with distinct amplitude and phases at both boundaries of the channel is given as

$$H_1\left(\widehat{X},t'\right)=-a_1\sin\left(\frac{2\pi\widehat{X}}{\lambda}-\frac{ct'}{\lambda}+\phi\right)-d-k'\widehat{X}, \tag{4.1}$$

$$H_2\left(\widehat{X},t'\right)=a_2\sin\left(\frac{2\pi\widehat{X}}{\lambda}-\frac{ct'}{\lambda}\right)+d+k'\widehat{X}, \tag{4.2}$$

where $\phi \in [0, \pi]$ represents the phase difference and amplitudes of the waves are a_1, a_2 . Keep in mind, waves are in phase when $\phi = \pi$, while waves out of phase are designated by $\phi = 0$. Furthermore d_1 , d_2 , a_1 , a_2 and ϕ satisfy the condition

$$a_1^2 + a_1^2 + 2a_1 a_1 \cos\phi \le (2d)^2 .$$

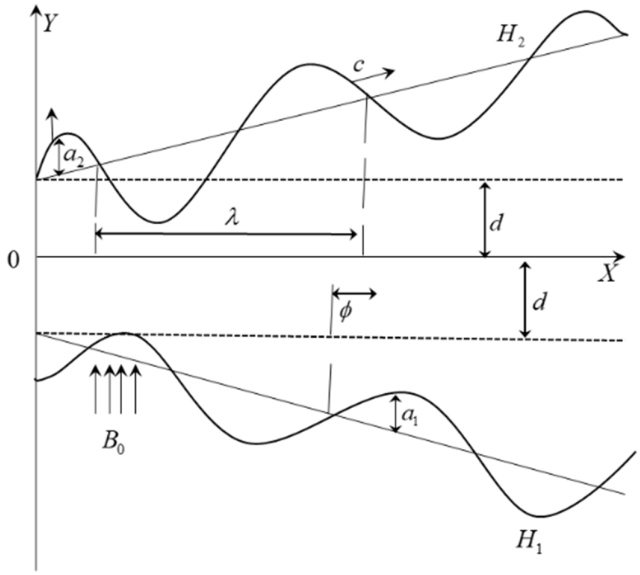

Figure 4.1: Problems geometry

The important equations to govern the flow in vector form are given as [18]:

$$\nabla . \boldsymbol{V} = 0, \tag{4.3}$$

$$\frac{d\boldsymbol{V}}{dt} = \frac{1}{\rho} div\boldsymbol{\tau} + \frac{1}{\rho}\mathbf{f}, \tag{4.4}$$

$$\frac{dT}{dt} = \frac{1}{\rho C_p}\boldsymbol{\tau} \cdot \boldsymbol{L} + \frac{\boldsymbol{\xi}}{\boldsymbol{\rho} C_p}\nabla^2 T - \frac{1}{\rho C_p}\nabla \cdot \boldsymbol{q}_r . \tag{4.5}$$

where d/dt designates the material derivative, $\boldsymbol{\tau}$ signifies the Cauchy stress tensor and $\boldsymbol{V}$ indicates the velocity vector.

The (JS) material has the subsequent mathematical illustration for its extra stress tensor [18]: which is defined in chapter one Eqs. (1.16) -(1.18).

Notice that the current model diminishes to fluid model given by Maxwell for e=1 and $\mu = 0$, we attain the basic NS model.

The velocity for 2-D unsteady flow is defined as:

$$\boldsymbol{V} = \left[\widehat{U}\left(\widehat{X},\widehat{Y},t'\right),\widehat{V}\left(\widehat{X},\widehat{Y},t'\right),0\right]. \tag{4.6}$$

The vector equations in components form are given by:

$$\widehat{U}_{\widehat{X}} + \widehat{V}_{\widehat{Y}} = 0, \tag{4.7}$$

$$\rho\left(\widehat{U}_{t'} + \widehat{U}\widehat{U}_{\widehat{X}} + \widehat{V}\widehat{U}_{\widehat{Y}}\right) = \left(\widehat{S}_{\widehat{X}\widehat{X}}\right)_{\widehat{X}} + \left(\widehat{S}_{\widehat{X}\widehat{Y}}\right)_{\widehat{Y}} - \widehat{P}_{\widehat{X}} + \mu\left(\widehat{U}_{\widehat{X}\widehat{X}} + \widehat{U}_{\widehat{Y}\widehat{Y}}\right) - \sigma B_0{}^2\widehat{U}, \tag{4.8}$$

$$\rho\left(\widehat{V}_{t'} + \widehat{U}\widehat{V}_{\widehat{X}} + \widehat{V}\widehat{V}_{\widehat{Y}}\right) = \left(\widehat{S}_{\widehat{Y}\widehat{Y}}\right)_{\widehat{X}} + \left(\widehat{S}_{\widehat{X}\widehat{Y}}\right)_{\widehat{Y}} - \widehat{P}_{\widehat{Y}} + \mu\left(\widehat{V}_{\widehat{X}\widehat{X}} + \widehat{V}_{\widehat{Y}\widehat{Y}}\right), \tag{4.9}$$

$$\begin{aligned} 2\eta\widehat{U}_{\widehat{X}} = \widehat{S}_{\widehat{X}\widehat{X}} - 2em\widehat{S}_{\widehat{X}\widehat{X}}\widehat{U}_{\widehat{X}} + m\left[\left(\widehat{S}_{\widehat{X}\widehat{X}}\right)_{t'} + \widehat{U}\left(\widehat{S}_{\widehat{X}\widehat{X}}\right)_{\widehat{X}} + \widehat{V}\left(\widehat{S}_{\widehat{X}\widehat{X}}\right)_{\widehat{Y}}\right] \\ + m\left[(1-e)\widehat{V}_{\widehat{X}} - (1+e)\widehat{U}_{\widehat{X}}\right]\widehat{S}_{\widehat{X}\widehat{X}}, \end{aligned} \tag{4.10}$$

$$\begin{aligned} \eta\left(\widehat{U}_{\widehat{Y}} + \widehat{V}_{\widehat{X}}\right) = \widehat{S}_{\widehat{X}\widehat{Y}} + m\widehat{S}_{\widehat{X}\widehat{Y}}\left[\left(\widehat{S}_{\widehat{X}\widehat{Y}}\right)_{t'} + \widehat{U}\left(\widehat{S}_{\widehat{X}\widehat{Y}}\right)_{\widehat{X}} + \widehat{V}\left(\widehat{S}_{\widehat{X}\widehat{Y}}\right)_{\widehat{Y}}\right] \\ + \frac{m}{2}\widehat{S}_{\widehat{X}\widehat{X}}\left[(1-e)\widehat{U}_{\widehat{Y}} - (1-e)\widehat{V}_{\widehat{X}}\right] + \frac{m}{2}\widehat{S}_{\widehat{Y}\widehat{Y}}\left[(1-e)\widehat{V}_{\widehat{X}} - (1-e)\widehat{U}_{\widehat{Y}}\right], \end{aligned} \tag{4.11}$$

$$\begin{aligned} 2\eta\widehat{V}_{\widehat{Y}} = \widehat{S}_{\widehat{Y}\widehat{Y}} - 2em\widehat{S}_{\widehat{Y}\widehat{Y}}\widehat{V}_{\widehat{Y}} + m\left[\left(\widehat{S}_{\widehat{Y}\widehat{Y}}\right)_{t'} + \widehat{U}\left(\widehat{S}_{\widehat{Y}\widehat{Y}}\right)_{\widehat{X}} + \widehat{V}\left(\widehat{S}_{\widehat{Y}\widehat{Y}}\right)_{\widehat{Y}}\right] \\ + m\left[(1-e)\widehat{U}_{\widehat{Y}} - (1-e)\widehat{V}_{\widehat{X}}\right]\widehat{S}_{\widehat{X}\widehat{Y}}, \end{aligned} \tag{4.12}$$

$$\rho C_p\left(T_{t'} + \widehat{U}T_{\widehat{X}} + \widehat{V}T_{\widehat{Y}}\right) = \xi\left(T_{\widehat{X}\widehat{X}} + T_{\widehat{Y}\widehat{Y}}\right) + \left(\widehat{U}_{\widehat{Y}} + \widehat{V}_{\widehat{X}}\right)\widehat{S}_{\widehat{X}\widehat{Y}} + \widehat{S}_{\widehat{Y}\widehat{Y}}\widehat{V}_{\widehat{Y}} + \widehat{S}_{\widehat{X}\widehat{X}}\widehat{U}_{\widehat{X}} - (q_r)_{\widehat{Y}}. \tag{4.13}$$

Defining the following dimensionless quantities

$$M = \sqrt{\sigma/\mu}B_0 d,\ \ Br = Ec\,\mathrm{Pr},\quad q_r = -\frac{16\sigma^* T_0^3}{3k^*}T_{\widehat{Y}},\ \ \theta = \frac{T - T_0}{T_1 - T_0}. \tag{4.14}$$

Invoking Eq. (3.12) and dimensionless quantities in Eq. (4.14) into Eqs. (4.7) - (4.13) and introducing stream functions $u = \psi_y, v = -\delta\psi_x$, we have

$$Re\delta\left(\psi_y\psi_{xy} - \psi_x\psi_{yy}\right) + M^2\psi_y + p_x\left(\frac{\mu+\eta}{\mu}\right) = \delta\left(s_{xx}\right)_x + \left(s_{xy}\right)_y + \left(\delta^2\psi_{xxy} + \psi_{yyy}\right), \tag{4.15}$$

$$-Re\delta^3\left(\psi_y\psi_{xx}-\psi_x\psi_{xy}\right)=-p_y\left(\frac{\mu+\eta}{\mu}\right)+\delta^2\left(s_{yx}\right)_x+\delta\left(s_{yy}\right)_y-\delta^2\left(\delta^2\psi_{xxx}+\psi_{xyy}\right), \quad (4.16)$$

$$\left(\frac{2\eta\delta}{\mu}\right)\psi_{xy}+2ems_{xx}We\delta\psi_{xy}=s_{xx}+We\delta\left[\psi_y\left(s_{xx}\right)_x-\psi_x\left(s_{xx}\right)_y\right] \quad (4.17)$$
$$-Wes_{xy}\left[\delta^2\left(1-e\right)\psi_{xx}+\left(1+e\right)\psi_{yy}\right],$$

$$\frac{\eta}{\mu}(\psi_{yy}-\delta^2\psi_{xx})=s_{xy}+We\delta\left[\psi_y(s_{xy})_x-\psi_x(s_{xy})_y\right] \quad (4.18)$$
$$+\frac{We}{2}s_{xx}\left[\left(1-e\right)\psi_{yy}+\delta^2\left(1+e\right)\psi_{xx}\right]-\frac{We}{2}\left[\delta^2(1-e)\psi_{xx}+(1+e)\psi_{yy}\right]s_{yy},$$

$$-\left(\frac{2\eta\delta}{\mu}\right)\psi_{xy}=s_{xy}+2eWe\delta s_{yy}\psi_{xy}+We\delta\left[\psi_y(s_{yy})_x-\psi_x(s_{yy})_y\right]+ \quad (4.19)$$
$$Wes_{xy}\left[\left(1-e\right)\psi_{yy}+\left(1+e\right)\delta^2\psi_{xx}\right],$$

$$\Pr\mathrm{Re}\,\delta\left(\psi_y\theta_x-\psi_x\theta_y\right)=\left(\theta_{yy}+\delta^2\theta_{xx}\right)+B_r\begin{pmatrix}\delta s_{xx}\psi_{xy}-\delta\psi_{xy}s_{yy}\\+s_{xy}\left(\psi_{yy}-\delta^2\psi_{xx}\right)\end{pmatrix}+Rd\theta_{yy}. \quad (4.20)$$

Utilizing approximation theory of lubrication i.e ($\mathrm{Re}\to 0$ and $\delta<<1$), Eqs. (4.15) -(4.20) turns into:

$$\left(\frac{\mu+\eta}{\mu}\right)p_x=(s_{xy})_y+\psi_{yyy}-M^2\psi_y, \quad (4.21)$$

$$p_y=0, \quad (4.22)$$

$$s_{xx}=We\left(1+e\right)\psi_{yy}s_{xy}, \quad (4.23)$$

$$\frac{\eta}{\mu}\psi_{yy}=s_{xy}+\frac{We}{2}\left(1-e\right)\psi_{yy}s_{xx}-\frac{We}{2}\left(1+e\right)\psi_{yy}s_{yy}, \quad (4.24)$$

$$s_{yy}=-We\left(1-e\right)\psi_{yy}s_{xy}, \quad (4.25)$$

$$\theta_{yy}=\frac{B_rs_{xy}\psi_{yy}}{\left(1+Rd\right)} \quad (4.26)$$

Removal of pressure from Eqs. (4.21) and (4.22), we have

$$\left(s_{xy}\right)_{yy}+\psi_{yyyy}-M^2\psi_{yy}=0. \quad (4.27)$$

Invoking Eqs. (4.23), (4.25) into Eq. (4.24), we have

$$s_{xy} = \frac{\left(\frac{\eta}{\mu}\right)\psi_{yy}}{1+We^2\left(1-e^2\right)\left(\psi_{yy}\right)^2}. \tag{4.28}$$

Eq. (4.28) allows Eqs. (4.21), (4.26), and (4.27) to be written in the following form

$$\frac{\partial^2}{\partial y^2}\left[\frac{\left(\frac{\eta}{\mu}+1\right)\psi_{yy}+We^2\left(1-e^2\right)\left(\psi_{yy}\right)^3}{1+We^2(1-e^2)\left(\psi_{yy}\right)^2}\right] = M^2\psi_{yy}, \tag{4.29}$$

$$\left(\frac{\mu+\eta}{\mu}\right)p_x = \frac{\partial}{\partial y}\left[\frac{\left(\frac{\eta}{\mu}\right)\psi_{yy}}{1+We^2\left(1-e^2\right)\left(\psi_{yy}\right)^2}\right]+\psi_{yyy} = M^2\psi_y, \tag{4.30}$$

$$\theta_{yy} = \frac{Br\left(\frac{\eta}{\mu}\right)\psi^2{}_{yy}}{\left(1+Rd\right)\left(1+We^2\left(1-e^2\right)\left(\psi_{yy}\right)^2\right)}. \tag{4.31}$$

The transformed boundary conditions are

$$\begin{aligned} &\psi = \frac{F}{2}, \quad \psi_y+\beta\psi_{yy}=0, \quad \theta=0 \quad \text{at} \quad y=h_1, \\ &\psi = -\frac{F}{2}, \quad \psi_y-\beta\psi_{yy}=0, \quad \theta=1 \quad \text{at} \quad y=h_2. \end{aligned} \tag{4.32}$$

4.3. Solution of the problem

After using binomial for small We^2, Eqs. (4.29), (4.30) and (4.31), may be simplified.

$$\left[\psi_{yy}+We^2\alpha\left(\psi_{yy}\right)^3\right]_{yy} - M^2\psi_{yy} = 0, \tag{4.33}$$

$$p_x = \psi_{yyy}+\left[We^2\alpha\left(\psi_{yy}\right)^3\right]_y - M^2\psi_y = 0, \tag{4.34}$$

$$\theta_{yy} = \left[\frac{Br\left(\frac{\eta}{\mu}\right)\psi^{2}{}_{yy}}{(1+Rd)\left(1+We^{2}\left(1-e^{2}\right)\left(\psi_{yy}\right)^{2}\right)} \right], \tag{4.35}$$

where $\alpha = \dfrac{\left(e^{2}-1\right)\eta}{(\eta+\mu)}$,

Since Eqs. (4.33) -(4.35) are highly nonlinear which are difficult to solve them analytically. So, using the regular perturbation method, approximate results are achieved. For perturbation solution, we express ψ, p_x and θ as

$$\begin{aligned} \psi &= \psi_0 + We^2\psi_1, \\ p_x &= p_{0x} + We^2 p_{1x}, \\ \theta &= \theta_0 + We^2\theta_1. \end{aligned} \tag{4.36}$$

Invoking Eq. (4.36) in Eqs. (4.33) -(4.35) and competing the same exponents of We^2, we have the subsequent systems.

0th -order system

$$\psi_{0yyyy} = M^2\psi_{0yy}, \tag{4.37}$$

$$p_{0x} = \psi_{0yyy} - M^2\psi_{0y}, \tag{4.38}$$

$$\theta_{0yy} = \frac{\eta Br}{\mu(1+Rd)}\psi^{2}{}_{0yy}, \tag{4.39}$$

$$\begin{aligned} &\psi_0 = \frac{F}{2}, \quad \psi_{1y} + \beta\psi_{1yy} = 0, \quad \theta_0 = 0 \quad \text{at} \quad y = h_1, \\ &\psi_0 = -\frac{F}{2} \quad \psi_{1y} - \beta\psi_{1yy} = 0, \quad \theta_0 = 1 \quad \text{at} \quad y = h_2. \end{aligned} \tag{4.40}$$

1st -order system

$$\psi_{1yyyy} = -\alpha\left[(\psi^{2}{}_{0yy})^{3}\right] + M^{2}\psi_{1yy}, \tag{4.41}$$

$$p_{1x} = \psi_{1yyy} + \alpha\left[(\psi^{2}{}_{0yy})^{3}\right]_y - M^{2}\psi_{1y}, \tag{4.42}$$

$$\theta_{1yy}=\left[\frac{Br\left(\frac{\eta}{\mu}\right)\psi^{2}{}_{1yy}}{(1+Rd)(1-e^{2})\left(\psi_{0yy}\right)^{2}}\right], \tag{4.43}$$

$$\begin{aligned}&\psi_1=\frac{F}{2}, \quad \psi_{1y}+\beta\psi_{1yy}=0, \quad \theta_1=0 \quad \text{at} \quad y=h_1,\\ &\psi_1=-\frac{F}{2} \quad \psi_{1y}-\beta\psi_{1yy}=0, \quad \theta_1=1 \quad \text{at} \quad y=h_2.\end{aligned} \tag{4.44}$$

After resolving the aforementioned systems, we arrive at the formulas for the stream function, axial velocity, pressure, and temperature.

$$\psi=\frac{1}{8M^{2}}e^{-3My}\begin{pmatrix}8e^{2My}M\left(B_3e^{My}M-C_2We^{2}+e^{My}\left(C_1e^{My}We^{2}+C_4MWe^{2}+B_4My\right)\right)\\+3B_2{}^{3}MWe^{2}\alpha-3B_1{}^{3}\mathrm{e}^{6My}MWe^{2}\alpha+8B_2e^{2My}+8B_1e^{4My}-\\6B_1{}^{2}B_2\mathrm{e}^{4My}MWe^{2}\left(-3+2My\right)\alpha-6B_1B_2{}^{2}\mathrm{e}^{2My}MWe^{2}\left(3+2My\right)\alpha\end{pmatrix}, \tag{4.45}$$

$$u=\frac{1}{8M}\mathrm{e}^{-3My}\begin{pmatrix}8\mathrm{e}^{2My}M\left(B_4\mathrm{e}^{My}+\left(C_2+C_1\mathrm{e}^{2My}\right)We^{2}\right)-9B_2{}^{3}MWe^{2}\alpha\\-9B_1{}^{3}\mathrm{e}^{6My}MWe^{2}\alpha+8B_1\mathrm{e}^{4My}+6B_1B_2{}^{2}\mathrm{e}^{2My}MWe^{2}\left(1+2My\right)\alpha\\-2B_2\mathrm{e}^{2My}\left(4+3B_1{}^{2}\mathrm{e}^{2My}MWe^{2}\left(-1+2My\right)\alpha\right)\end{pmatrix}, \tag{4.46}$$

$$\begin{aligned}&p_x=B_4M^{2}\left(h_1-h_2\right)\\&+\frac{1}{8}We^{2}\begin{pmatrix}8C_4h_1M^{2}-8C_4h_2M^{2}+9B_1{}^{3}\mathrm{e}^{3h_2M}\left(1-3M\right)\alpha+9B_1{}^{3}\mathrm{e}^{3h_1M}\left(3M-1\right)\alpha\\-9B_2{}^{3}\mathrm{e}^{-3h_1M}\left(3M+1\right)\alpha+9B_2{}^{3}\mathrm{e}^{-3h_2M}\left(3M+1\right)\alpha\\+2\mathrm{e}^{h_1M}\left(-4C_1\left(M-1\right)+3B_1{}^{2}B_2\left(1+M+2h_1\left(M-1\right)M\right)\alpha\right)\\-2\mathrm{e}^{h_2M}\left(-4C_1\left(M-1\right)+3B_1{}^{2}B_2\left(1+M+2h_2\left(M-1\right)M\right)\alpha\right)\\-2\mathrm{e}^{-h_1M}\left(-4C_2\left(M+1\right)+3B_1B_2{}^{2}\left(-1+M-2h_1M\left(M+1\right)\right)\alpha\right)\\+2\mathrm{e}^{-h_2M}\left(-4C_2\left(M+1\right)+3B_1B_2{}^{2}\left(-1+M-2h_2M\left(M+1\right)\right)\alpha\right)\end{pmatrix},\end{aligned} \tag{4.47}$$

$$\theta = B_5 + C_5 We^2 + B_6 y + C_6 We^2 y - \frac{ABr\left(B_2{}^2 \mathrm{e}^{-2My} + B_1{}^2 \mathrm{e}^{2My} + 4B_1 B_2 M^2 y^2\right)}{4M\left(M + M\,\mathrm{Pr}\,Rd\right)}$$

$$+ \frac{1}{8M\left(M + M\,\mathrm{Pr}\,Rd\right)} ABrWe^2 \tag{4.48}$$

$$\begin{pmatrix} B_2{}^3 \mathrm{e}^{-3My}\alpha + B_1{}^3 \mathrm{e}^{3My}\alpha - 2\mathrm{e}^{My}\left(4C_1 + B_1\begin{pmatrix} 4\left(e^2-1\right)M^2 + 15B_1B_2\alpha \\ -6B_1B_2My\alpha \end{pmatrix}\right) \\ -2\mathrm{e}^{-My}\left(4C_2 + B_2\begin{pmatrix} 4\left(e^2-1\right)M^2 + 15B_1B_2\alpha \\ +6B_1B_2My\alpha \end{pmatrix}\right) \end{pmatrix},$$

At a fixed location $\widehat{X}$, the time averaged flow is defined as

$$Q = \int_0^T Q dt\,. \tag{4.49}$$

We discover

$$Q = q + a_1 csin\left[\frac{2\pi}{\lambda}\left(\widehat{X} - ct\right) + \phi\right] + a_2 csin\left[\frac{2\pi}{\lambda}\left(\widehat{X} - ct\right)\right],$$

where $q = \int_{H_1}^{H_2} \overline{u}\left(\overline{x}, \overline{y}\right) d\overline{y}$ represents the dimensional volume flow rate in the wave frame.

By the meanings of dimensionless mean flows Θ in the wave frame and F in the laboratory frame are described as

$$F = \frac{Q}{cd}, \qquad \Theta = \frac{q}{cd}\,.$$

We find that

$$F\left(x,t\right) = a\sin 2\pi\left(x-t\right) + b\sin\left[\phi + 2\pi\left(x-t\right)\right] + \Theta,$$

In which $F = \int_{h_1}^{h_2} u dy$.

The usual increase in Δp over one wavelength period is given by

$$\Delta p = \int_0^1 \int_0^1 \left(\frac{dp}{dx}\right)_{y=0} dx dt\,. \tag{4.50}$$

The constant appearing in above equations are given in appendix.

4.4 Discussion of the findings

This section uses graphical findings to show how different variables affect velocity, pressure rise, temperature, and streamlines. The representation for Δp contains the integration of dp/dx which is difficult to integrate analytically. Therefore, the integral occurring in Eq. (4.50) has been estimated numerically utilizing MATHEMATICA through composite Simpson's rule. During this investigation, In order to facilitate computations, the following standard parametric values are used: $\beta = 0.01$, $M = 1$, $t = 0.2$, $a = 0.3$, $\Theta = 1.75$, $\mu = 0.3$, $B_r = 2$, $Rd = 0.2$, $\eta = 0.2$, $e = 0.2$ $k = 0.2$, $x = 0.4$, $\phi = \pi/4$ and $b = 0.2$.

Figure 4.2 (a-d) is intended to examine and discuss the effects of substantial parameters on the momentum profile. u. Figure 4.2a is displayed to observe the Hartmann parameter impressions (M) on momentum transfer. It is shown that as the value of (M)increases, the velocity of the liquid decreases. Physically, increasing the strength of a magnetic field enhances the Lorentz force, causing fluid materials to encounter more resistance, reducing liquid velocity. This perception has a significant impact in the medication field, where the local energy augments in the existence of a structured external magnetic field, which aids in the elimination of tumor cells. Figure 4.2b depicts the effect of the slip parameter (β) on liquid velocity. This graph shows that increasing behavior in slip parameter cause a decrease the liquid velocity in the center of channel. Figure 4.2c portrays the behvavior in momentum profile for various values of (We). The liquid velocity decreases as (We) increases. Figure 4.2d examines the deviations in the momentum profile for different values of (e). Figure 4.2d shows that higher values of (e) increase liquid velocity.

The influences of governing variable quantities on temperature are available in Figure 4.3(a-c). In Figure 4.3a we depict the effects of (Br) on temperature profile. It is notable that temperature improves with enhancing amounts of (Br). Physically, the (Br) boosts the conflict to the flow for the reason that of its shear strength, which in turn leads

to an improvement in intensity due to the viscid dissipation influence. So, rises the fluid temperature. Figure 4.3b explains the impact of (Rd) on temperature distribution. The graph signifies that liquid temperature reduces for boosting quantities of the parameter (Rd). Figure 4.3c demonstrates the variation of the (We) on the fluid temperature. We can examine from this graph; fluid temperature enhances for greater values of the (We). Figure 4.4(a-d) exhibits a graph of the Δp vs. the change in time-average flux Q. Figure 4.4(a-d) demonstrate pumping zones such as peristaltic injecting $(Q > 0, \Delta p > 0)$ enhanced driving $(Q > 0, \Delta p < 0)$, and backward injecting $(Q < 0, \Delta p > 0)$). Figure 4.4a is portrayed to perceive the influences of (M) on pressure gradient profile Δp. It is discovered since this diagram that the injecting rate shows a decrement with increasing (M) in the enhanced driving region, whereas the inverse trend is scrutinized in the backward driving zone. The graph illustrated in Figure 4.4b displays the deviation of rise in pressure with different values of slip parameter. From this graph, we perceive that the injecting rate is increased with slip parameter in the augmented driving segment and reduces in the backward driving zone. The influence of (e) on Δp is displayed in Figure 4.4c. This graph demonstrates greater values of (e) increasing the Δp in the backward driving zone. Figure 4.4d is graphed to depict the deviation in pressure rise for various values of We. We can note that pressure in the retrograde pumping portion is reduced with the changing behavior of We.

The process of trapping, in which a bolus is moved along a peristaltic movement at the speed of the wave and is pushed forward, is one of the most exciting aspects of fluid transportation. Figure 4.5 produces the variation of (M) on ψ. It can be seen from this Figure that an improvement in (M) results in a decrease in the trapping bolus. The Lorentz forces, which serve as a retarding force, are partially responsible for this decline in the size of the bolus. The effect of the flow average flow Q on the streamlines is presented in Figure 4.6 and examine that the trapped bolus is increased in magnitude as Q improves and more trapped bolus appears with rising values Q. Figure 4.7 illustrates

the difference in (We) on ψ . The plots depict that when (We) increases then the confining bolus also increases.

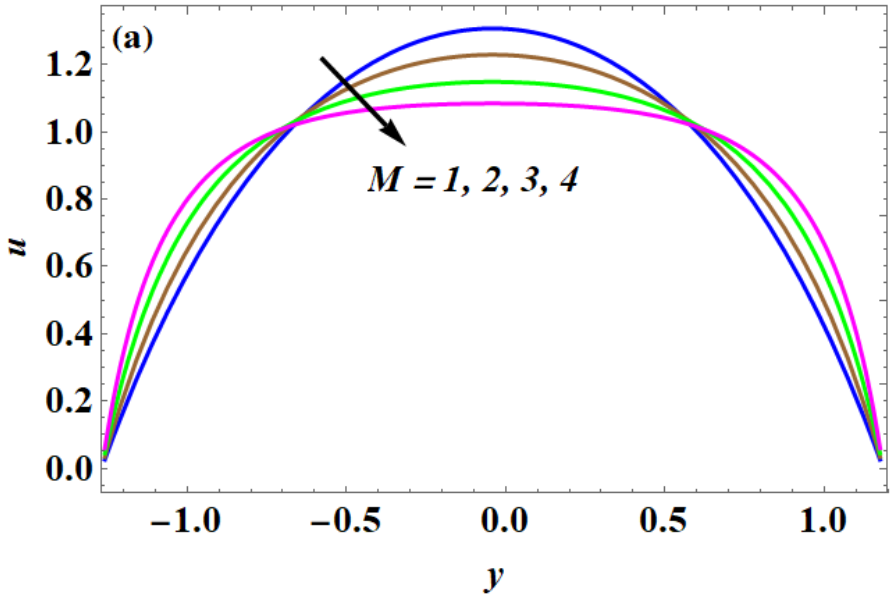

Figure 4.2(a): Effects of M on axial velocity.

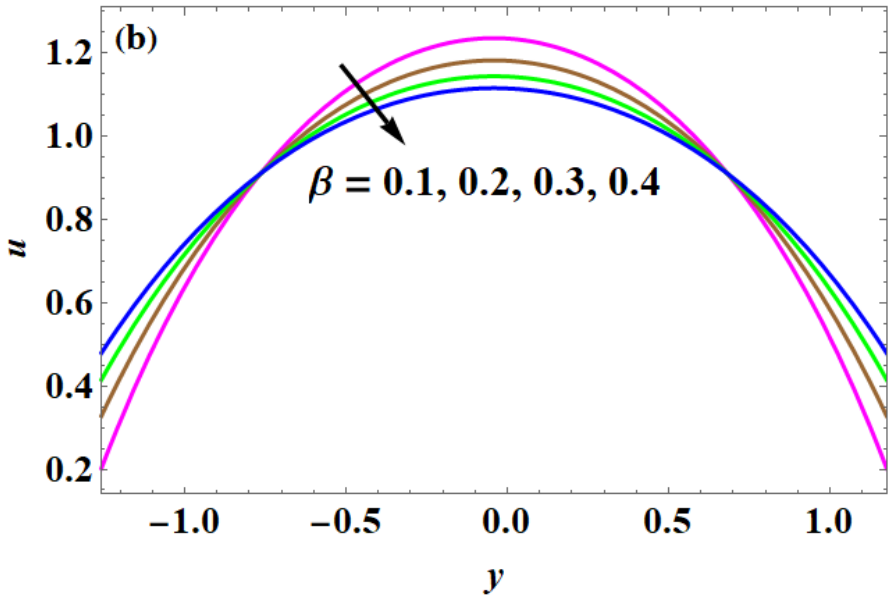

Figure 4.2(b): Effects of β on axial velocity.

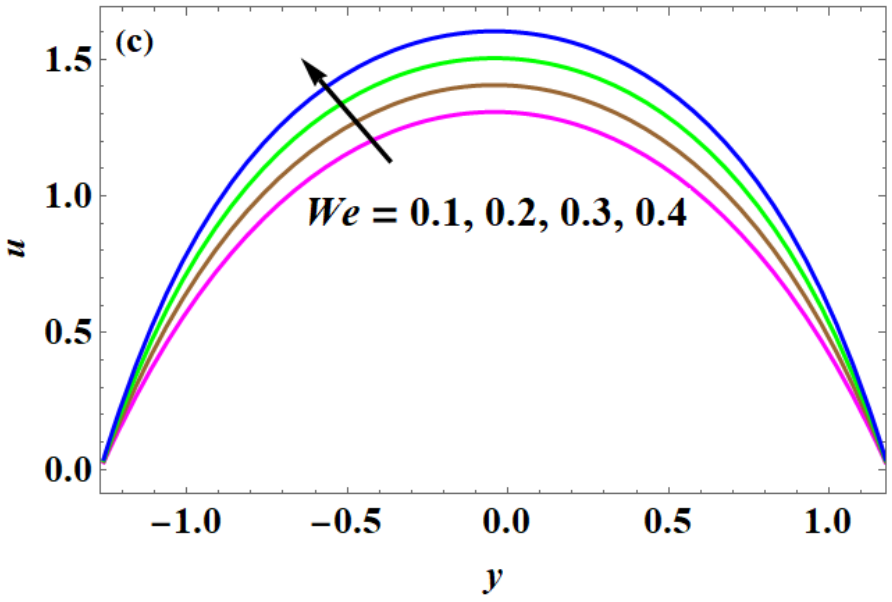

Figure 4.2(c): Effects of We on axial velocity.

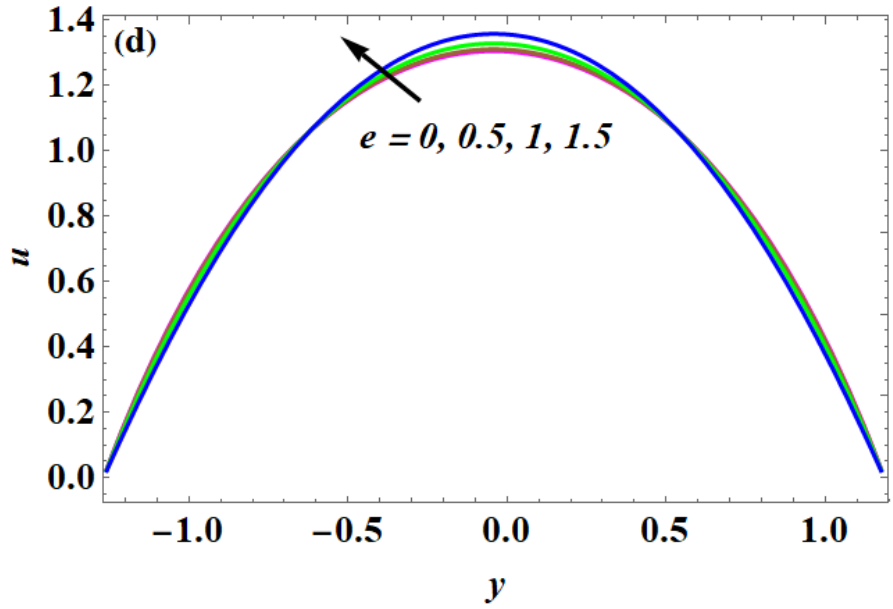

Figure 4.2(d): Effects of e on axial velocity

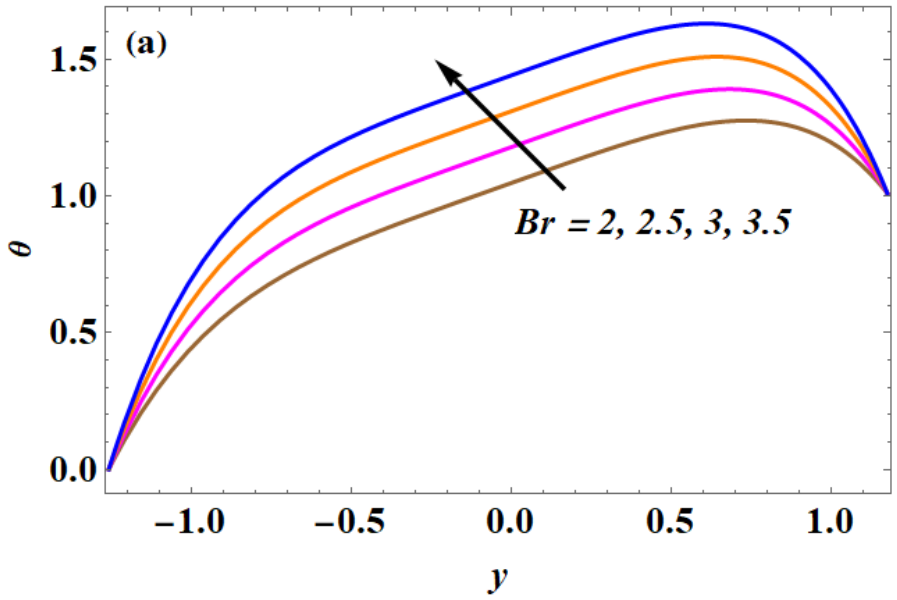

Figure 4.3(a): Effects of Br on temperature.

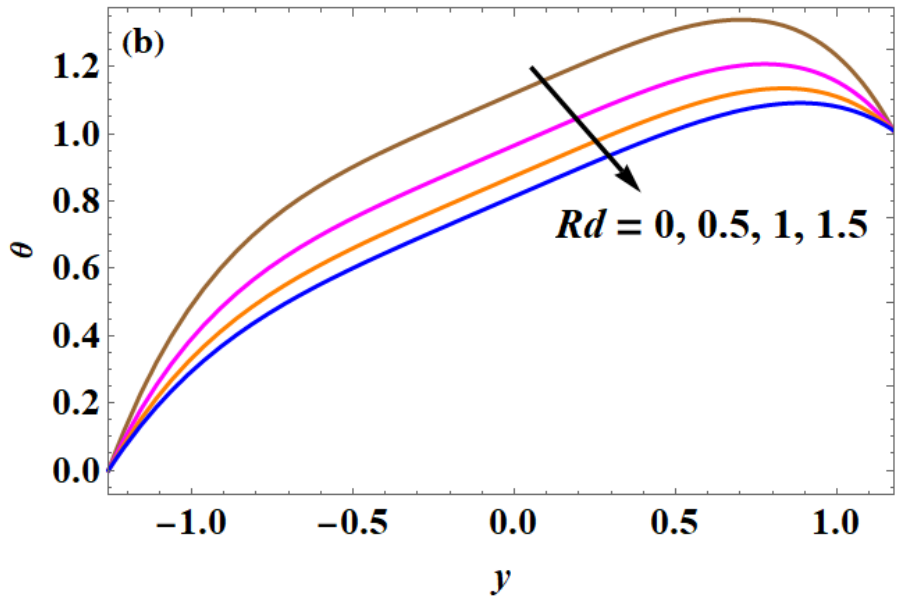

Figure 4.3(b): Effects of Rd on temperature.

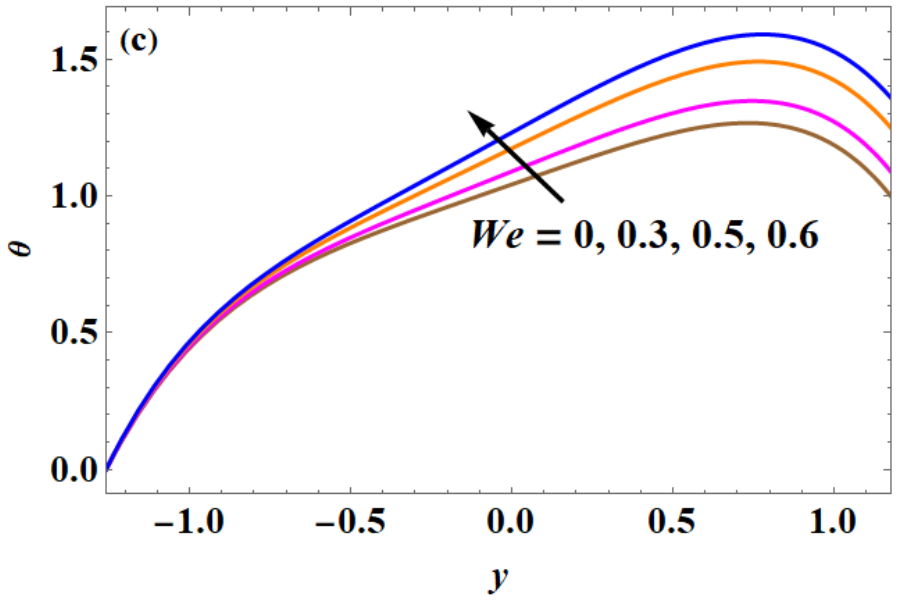

Figure 4.3(c): Effects of We on temperature.

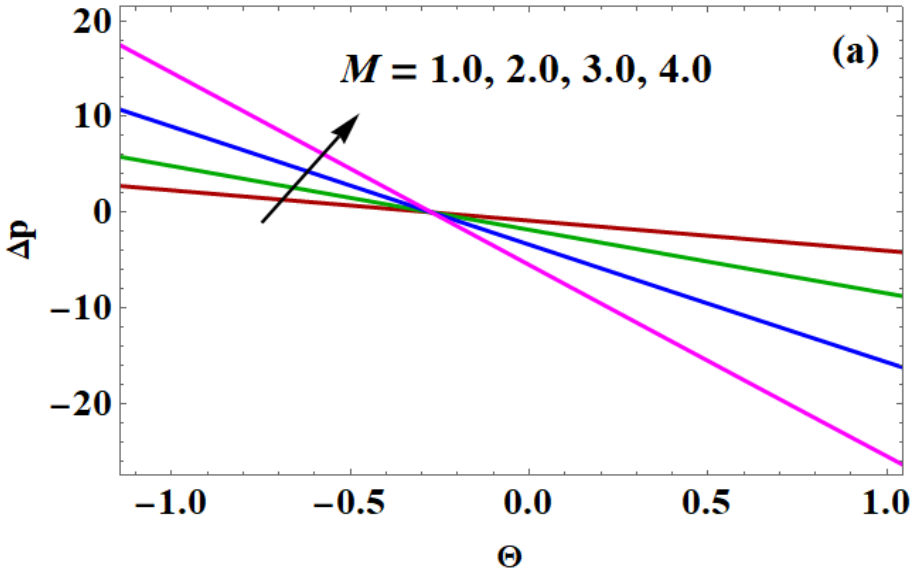

Figure 4.4(a): Effects of M on pressure.

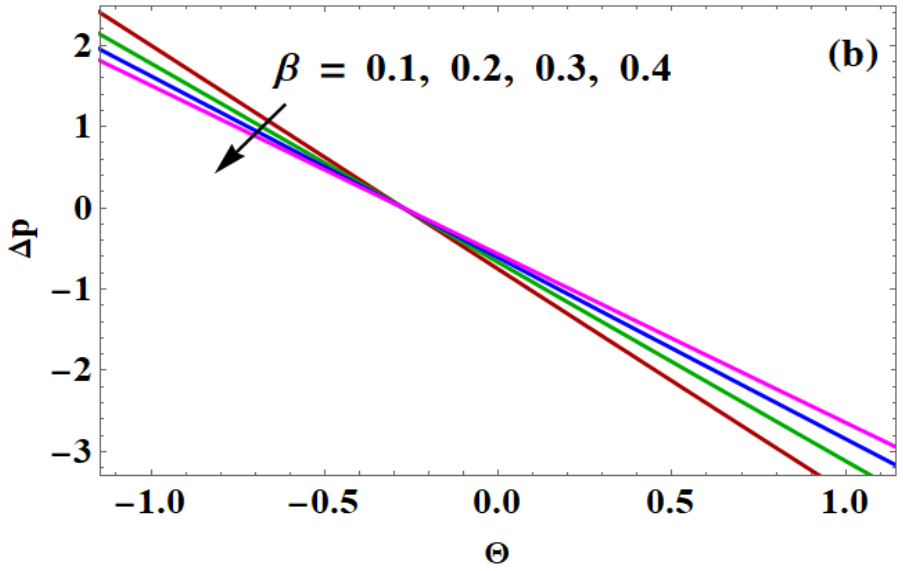

Figure 4.4(b): Effects of β on pressure.

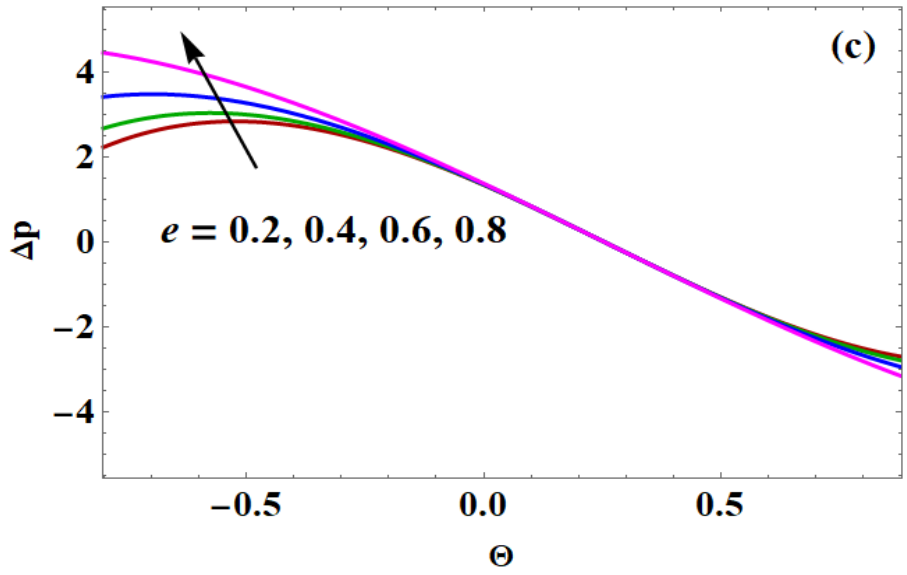

Figure 4.4(c): Effects of e on pressure.

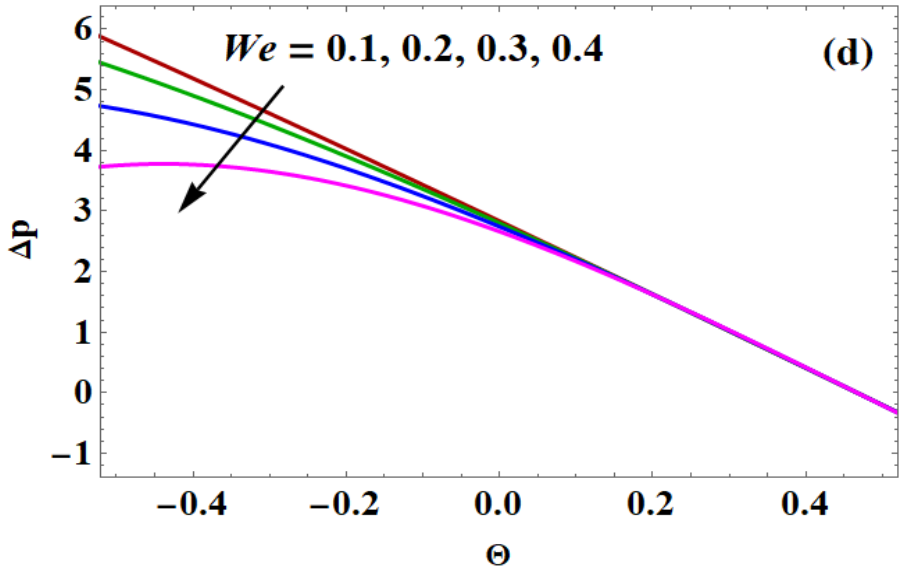

Figure 4.4(d): Effects of We on pressure.

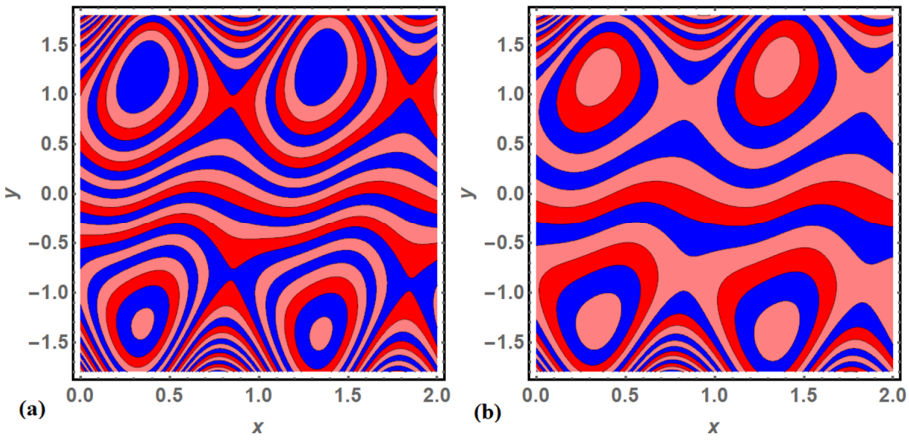

Figure 4.5: Streamlines for various values of (a) $M = 1$ (b) $M = 2$.

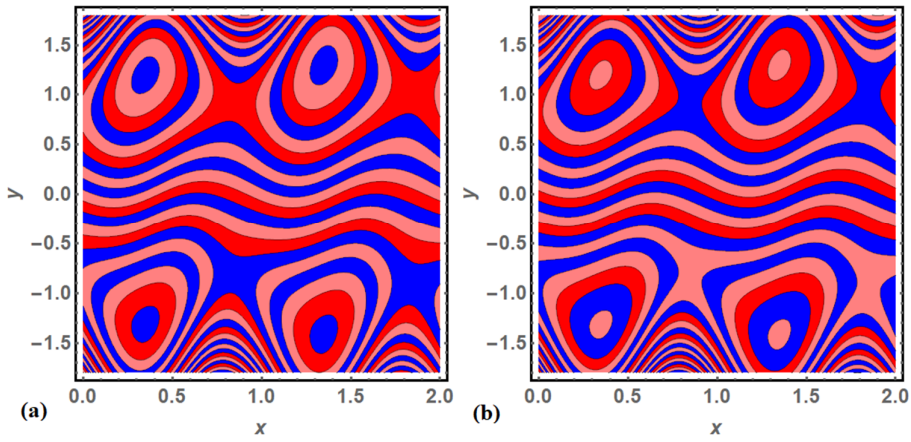

Figure 4.6: Streamlines for various values of (a) $Q = 1.2$, (b) $Q = 1.4$.

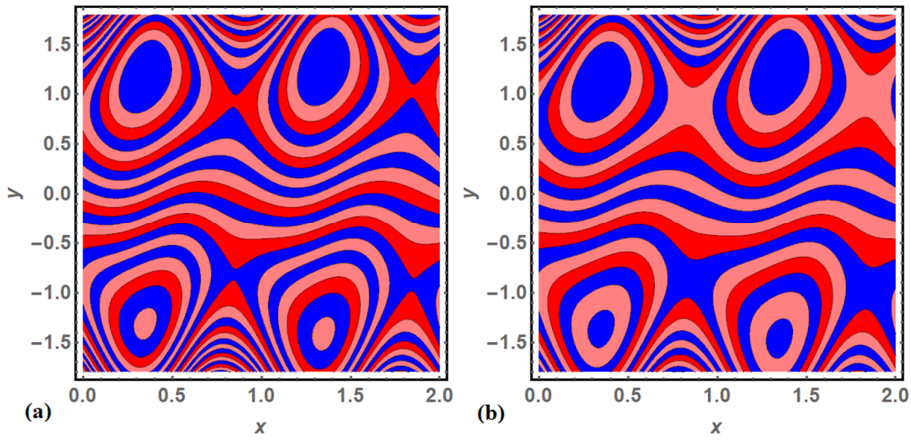

Figure 4.7: Streamlines for various values of (a) $We = 0$, (b) $We = 0.2$.

CHAPTER 5

CONCLUSION AND FUTURE WORK

5.1 Conclusion

In this thesis, we studied, the peristaltic transport of Johnson-Segalman fluid in a tapered asymmetric channel, with viscous dissipation and effects of thermal radiation. We built a mathematical model. The tapered asymmetric channel is created by varying the amplitudes and phase of peristaltic wave trains over nonuniform walls. Approximations with a long wavelength and low Reynolds number have been used. The expressions for stream function, axial velocity, temperature profile and pressure gradient were computed using a regular perturbation approach. It is addressed how the fluid's rheological characteristics interact with peristaltic transport. The variations of dissimilar flow parameters under the change of the present flow factors are well portrayed via graphic representations. The main observations are:

- The pressure falls with changing behavior of We in retrograde pumping portion however pressure rise improves in this region with improving magnetic number.
- An augmentation in the quantities of radiation parameter causes a decline in the liquid temperature.
- The number of trapped bolus diminishes with greater values of magnetic number.
- It has been discovered that as a and e increase, the average rise in pressure Δp increases, whereas k, ϕ and η decrease.
- It was also discovered that with rise in η, k, and Q, the momentum transport in axial direction is decreased.

5.2 Future work

For further work following may be considered

- The Johsnon-Segalman model can be studied with different geometries with different boundary conditions.
- Entropy generation also can be discussed
- Chemical reaction

APPENDIX

$$B_1 = -\frac{FM^2}{\mathrm{e}^{h_1 M}\left(2+\left(h_1-h_2\right)M\left(-1+M\beta\right)\right)+\mathrm{e}^{h_2 M}\left(-2-\left(h_1-h_2\right)M\left(1+M\beta\right)\right)},$$

$$B_2 = \frac{\mathrm{e}^{M\left(h_1+h_2\right)}FM^2}{\mathrm{e}^{Mh_1}\left(2+M\left(-1+M\beta\right)\left(h_1-h_2\right)\right)+\mathrm{e}^{Mh_2}\left(-2+M\left(1+M\beta\right)\left(-h_1+h_2\right)\right)},$$

$$B_3 = \frac{FM\left(\mathrm{e}^{Mh_1}\left(-1+M\beta\right)-\mathrm{e}^{Mh_2}\left(1+M\beta\right)\right)\left(h_1+h_2\right)}{2\mathrm{e}^{Mh_1}\left(2+M\left(-1+M\beta\right)\left(h_1-h_2\right)\right)+2\mathrm{e}^{Mh_2}\left(-2+M\left(1+M\beta\right)\left(-h_1+h_2\right)\right)},$$

$$B_4 = \frac{FM\left(\mathrm{e}^{Mh_1}\left(1-M\beta\right)+\mathrm{e}^{Mh_2}\left(1+M\beta\right)\right)}{\mathrm{e}^{Mh_1}\left(2+M\left(-1+M\beta\right)\left(h_1-h_2\right)\right)+\mathrm{e}^{Mh_2}\left(-2+M\left(1+M\beta\right)\left(-h_1+h_2\right)\right)},$$

$$C_1 = \frac{\left(\begin{array}{l}
\mathrm{e}^{-3M\left(h_1+h_2\right)}(-8\mathrm{e}^{3M\left(h_1+h_2\right)}FM^2\left(\mathrm{e}^{Mh_1}\left(-1+M\beta\right)+\mathrm{e}^{Mh_2}\left(1+M\beta\right)\right)+\alpha B_2^3(2\left(\mathrm{e}^{Mh_1}-\mathrm{e}^{Mh_2}\right)\\
\left(-\mathrm{e}^{M\left(2h_1+h_2\right)}M\beta-\mathrm{e}^{M\left(h_1+2h_2\right)}M\beta+\mathrm{e}^{3Mh_1}\left(-1+4M\beta\right)+\mathrm{e}^{3Mh_2}\left(1+4M\beta\right)\right)-3\mathrm{e}^{M\left(h_1+h_2\right)}\\
M(\mathrm{e}^{2Mh_2}\left(1+2M\beta-3M^2\beta^2\right)+\mathrm{e}^{2Mh_1}\left(-1+2M\beta+3M^2\beta^2\right))h_1+3\mathrm{e}^{M\left(h_1+h_2\right)}\\
M\left(\mathrm{e}^{2Mh_2}\left(1+2M\beta-3M^2\beta^2\right)+\mathrm{e}^{2Mh_1}\left(-1+2M\beta+3M^2\beta^2\right)\right)h_2)\\
+\mathrm{e}^{3M\left(h_1+h_2\right)}\alpha B_1^3(2\left(\mathrm{e}^{Mh_1}-\mathrm{e}^{Mh_2}\right)\left(\begin{array}{l}\mathrm{e}^{M\left(2h_1+h_2\right)}M\beta+\mathrm{e}^{M\left(h_1+2h_2\right)}M\beta+\\ \mathrm{e}^{3Mh_1}\left(-2+5M\beta\right)+\mathrm{e}^{3Mh_2}\left(2+5M\beta\right)\end{array}\right)\\
+3M\left(\mathrm{e}^{4Mh_1}\left(1-4M\beta+3M^2\beta^2\right)-\mathrm{e}^{4Mh_2}\left(1+4M\beta+3M^2\beta^2\right)\right)h_1\\
-3M\left(\mathrm{e}^{4Mh_1}\left(1-4M\beta+3M^2\beta^2\right)-\mathrm{e}^{4Mh_2}\left(1+4M\beta+3M^2\beta^2\right)\right)h_2)\\
-12\mathrm{e}^{2M\left(h_1+h_2\right)}\alpha B_1B_2^2(\mathrm{e}^{2Mh_1}+\mathrm{e}^{2Mh_2}-2\mathrm{e}^{M\left(h_1+h_2\right)}-2\mathrm{e}^{2Mh_1}M\beta+2\mathrm{e}^{2Mh_2}M\beta\\
+\mathrm{e}^{M\left(h_1+h_2\right)}M^2\left(-1+M^2\beta^2\right)h_1^2-4\mathrm{e}^{M\left(h_1+h_2\right)}M^2\beta h_2+\mathrm{e}^{M\left(h_1+h_2\right)}M^2\left(-1+M^2\beta^2\right)h_2^2-2\mathrm{e}^{M\left(h_1+h_2\right)}\\
M^2h_1\left(-2\beta+\left(-1+M^2\beta^2\right)h_2\right))+6\alpha B_1^2B_2(2\mathrm{e}^{5Mh_1+3Mh_2}M^2\left(-1+M\beta\right)^2h_1^2+\mathrm{e}^{3M\left(h_1+h_2\right)}\\
Mh_1(4\mathrm{e}^{M\left(h_1+h_2\right)}-\mathrm{e}^{2Mh_1}\left(7-8M\beta+M^2\beta^2\right)+\mathrm{e}^{2Mh_2}\left(3+4M\beta+M^2\beta^2\right)-2M\\
\left(\mathrm{e}^{2Mh_1}\left(-1+M\beta\right)^2+\mathrm{e}^{2Mh_2}\left(1+M\beta\right)^2\right)h_2)+\mathrm{e}^{3M\left(h_1+h_2\right)}(-16\mathrm{e}^{M\left(h_1+h_2\right)}+\mathrm{e}^{2Mh_1}\left(8-6M\beta\right)+\mathrm{e}^{2Mh_2}\left(8+6M\beta\right)\\
+M\left(4\mathrm{e}^{M\left(h_1+h_2\right)}+\mathrm{e}^{2Mh_1}\left(3-4M\beta+M^2\beta^2\right)-\mathrm{e}^{2Mh_2}\left(7+8M\beta+M^2\beta^2\right)\right)h_2+2\mathrm{e}^{2Mh_2}M^2\left(1+M\beta\right)^2h_2^2)))
\end{array}\right)}{\left(8\left(\mathrm{e}^{Mh_1}\left(-1+M\beta\right)+\mathrm{e}^{Mh_2}\left(1+M\beta\right)\right)\left(2\left(\mathrm{e}^{Mh_1}-\mathrm{e}^{Mh_2}\right)+M\left(\mathrm{e}^{Mh_1}\left(-1+M\beta\right)-\mathrm{e}^{Mh_2}\left(1+M\beta\right)\right)h_1+M\left(\mathrm{e}^{Mh_1}\left(1-M\beta\right)+\mathrm{e}^{Mh_2}\left(1+M\beta\right)\right)h_2\right)\right)},$$

$$C_2=\frac{\left(\begin{array}{l}
e^{-2M(h_1+h_2)}(-8e^{3M(h_1+h_2)}FM^2\left(e^{Mh_1}\left(-1+M\beta\right)+e^{Mh_2}\left(1+M\beta\right)\right)\\
+e^{3M(h_1+h_2)}\alpha B_1^3(-2\left(e^{Mh_1}-e^{Mh_2}\right)(-e^{M(2h_1+h_2)}M\beta-e^{M(h_1+2h_2)}M\beta\\
+e^{3Mh_1}\left(-1+4M\beta\right)+e^{3Mh_2}\left(1+4M\beta\right))+3e^{M(h_1+h_2)}M(e^{2Mh_2}\left(1+2M\beta-3M^2\beta^2\right)\\
+e^{2Mh_1}\left(-1+2M\beta+3M^2\beta^2\right))h_1-3e^{M(h_1+h_2)}M\left(e^{2Mh_2}\left(1+2M\beta-3M^2\beta^2\right)+e^{2Mh_1}\left(-1+2M\beta+3M^2\beta^2\right)\right)h_2)\\
+\alpha B_2^3(-2\left(e^{Mh_1}-e^{Mh_2}\right)\left(e^{M(2h_1+h_2)}M\beta+e^{M(h_1+2h_2)}M\beta+e^{3Mh_1}\left(-2+5M\beta\right)+e^{3Mh_2}\left(2+5M\beta\right)\right)\\
-3M\left(e^{4Mh_1}\left(1-4M\beta+3M^2\beta^2\right)-e^{4Mh_2}\left(1+4M\beta+3M^2\beta^2\right)\right)h_1+3M\left(e^{4Mh_1}\left(1-4M\beta+3M^2\beta^2\right)-e^{4Mh_2}\left(1+4M\beta+3M^2\beta^2\right)\right)h_2)\\
+12e^{3M(h_1+h_2)}\alpha B_1^2B_2(e^{2Mh_1}+e^{2Mh_2}-2e^{M(h_1+h_2)}-2e^{2Mh_1}M\beta+2e^{2Mh_2}M\beta+e^{M(h_1+h_2)}M^2\left(-1+M^2\beta^2\right)h_1^2\\
-4e^{M(h_1+h_2)}M^2\beta h_2+e^{M(h_1+h_2)}M^2\left(-1+M^2\beta^2\right)h_2^2-2e^{M(h_1+h_2)}M^2h_1\left(-2\beta+\left(-1+M^2\beta^2\right)h_2\right))\\
+6\alpha B_1B_2^2(-2e^{2M(h_1+2h_2)}M^2\left(1+M\beta\right)^2h_1^2+e^{2M(h_1+h_2)}Mh_1(4e^{M(h_1+h_2)}+e^{2Mh_1}\left(3-4M\beta+M^2\beta^2\right)\\
-e^{2Mh_2}\left(7+8M\beta+M^2\beta^2\right)+2M\left(e^{2Mh_1}\left(-1+M\beta\right)^2+e^{2Mh_2}\left(1+M\beta\right)^2\right)h_2)+e^{2M(h_1+h_2)}\\
\left(16e^{M(h_1+h_2)}-2e^{2Mh_2}\left(4+3M\beta\right)+e^{2Mh_1}\left(-8+6M\beta\right)-M\begin{pmatrix}-4e^{M(h_1+h_2)}+e^{2Mh_1}\left(7-8M\beta+M^2\beta^2\right)\\-e^{2Mh_2}\left(3+4M\beta+M^2\beta^2\right)\end{pmatrix}h_2-2e^{2Mh_1}M^2\left(-1+M\beta\right)^2h_2^2\right))
\end{array}\right)}{\left(8\left(e^{Mh_1}\left(-1+M\beta\right)+e^{Mh_2}\left(1+M\beta\right)\right)\left(-2e^{Mh_1}+2e^{Mh_2}+M\left(e^{Mh_1}\left(1-M\beta\right)+e^{Mh_2}\left(1+M\beta\right)\right)h_1+M\left(e^{Mh_1}\left(-1+M\beta\right)-e^{Mh_2}\left(1+M\beta\right)\right)h_2\right)\right)},$$

$$C_3=\frac{\left(\begin{array}{l}
e^{-3M(h_1+h_2)}(2e^{3M(h_1+h_2)}FM^3\left(-e^{2Mh_1}\left(-1+M\beta\right)^2+e^{2Mh_2}\left(1+M\beta\right)^2\right)\left(h_1+h_2\right)\\
-e^{3M(h_1+h_2)}\alpha B_1^3(\left(-e^{Mh_1}+e^{Mh_2}\right)\left(e^{Mh_1}+e^{Mh_2}\right)^2\left(-4e^{M(h_1+h_2)}M\beta+e^{2Mh_1}\left(-1+4M\beta\right)+e^{2Mh_2}\left(1+4M\beta\right)\right)\\
+e^{Mh_2}M\left(e^{4Mh_1}\left(-3+9M\beta\right)+e^{2M(h_1+h_2)}\left(2+2M\beta-4M^2\beta^2\right)+e^{4Mh_2}\left(1+5M\beta+4M^2\beta^2\right)\right)h_1\\
+e^{Mh_1}M\left(-3e^{4Mh_2}\left(1+3M\beta\right)-2e^{2M(h_1+h_2)}\left(-1+M\beta+2M^2\beta^2\right)+e^{4Mh_1}\left(1-5M\beta+4M^2\beta^2\right)\right)h_2)\\
+\alpha B_2^3(\left(e^{Mh_1}-e^{Mh_2}\right)\left(e^{Mh_1}+e^{Mh_2}\right)^2\left(-4e^{M(h_1+h_2)}M\beta+e^{2Mh_1}\left(-1+4M\beta\right)+e^{2Mh_2}\left(1+4M\beta\right)\right)\\
+e^{Mh_1}M\left(-3e^{4Mh_2}\left(1+3M\beta\right)-2e^{2M(h_1+h_2)}\left(-1+M\beta+2M^2\beta^2\right)+e^{4Mh_1}\left(1-5M\beta+4M^2\beta^2\right)\right)h_1\\
+e^{Mh_2}M\left(e^{4Mh_1}\left(-3+9M\beta\right)+e^{2M(h_1+h_2)}\left(2+2M\beta-4M^2\beta^2\right)+e^{4Mh_2}\left(1+5M\beta+4M^2\beta^2\right)\right)h_2)\\
-6\alpha B_1^2B_2(e^{3M(h_1+h_2)}\left(-e^{2Mh_1}+e^{2Mh_2}\right)\left(e^{Mh_1}\left(-1+2M\beta\right)+e^{Mh_2}\left(1+2M\beta\right)\right)\\
+2e^{5Mh_1+4Mh_2}M^2\left(-1+M\beta\right)h_1^2+e^{4Mh_1+3Mh_2}M(-2e^{M(h_1+h_2)}+e^{2Mh_2}\left(1-5M\beta-2M^2\beta^2\right)\\
+e^{2Mh_1}\left(1-3M\beta+2M^2\beta^2\right))h_2-2e^{4Mh_1+5Mh_2}M^2\left(1+M\beta\right)h_2^2+e^{3Mh_1+4Mh_2}Mh_1(-2e^{M(h_1+h_2)}+e^{2Mh_1}\left(1+5M\beta-2M^2\beta^2\right)\\
+e^{2Mh_2}\left(1+3M\beta+2M^2\beta^2\right)-2e^{Mh_1}M\left(e^{Mh_1}\left(-1+M\beta\right)-e^{Mh_2}\left(1+M\beta\right)\right)h_2))\\
+6e^{2M(h_1+h_2)}\alpha B_1B_2^2(\left(e^{2Mh_1}-e^{2Mh_2}\right)\left(e^{Mh_1}\left(-1+2M\beta\right)+e^{Mh_2}\left(1+2M\beta\right)\right)+2e^{M(h_1+2h_2)}M^2\left(1+M\beta\right)h_1^2\\
+e^{Mh_2}M\left(-2e^{M(h_1+h_2)}+e^{2Mh_1}\left(1+5M\beta-2M^2\beta^2\right)+e^{2Mh_2}\left(1+3M\beta+2M^2\beta^2\right)\right)h_2\\
-2e^{M(2h_1+h_2)}M^2\left(-1+M\beta\right)h_2^2+e^{Mh_1}Mh_1(-2e^{M(h_1+h_2)}+e^{2Mh_2}\left(1-5M\beta-2M^2\beta^2\right)\\
+e^{2Mh_1}\left(1-3M\beta+2M^2\beta^2\right)-2e^{Mh_2}M\left(e^{Mh_1}\left(1-M\beta\right)+e^{Mh_2}\left(1+M\beta\right)\right)h_2)))
\end{array}\right)}{\left(4M^2\left(e^{Mh_1}\left(-1+M\beta\right)+e^{Mh_2}\left(1+M\beta\right)\right)\left(-2e^{Mh_1}+2e^{Mh_2}+M\left(e^{Mh_1}\left(1-M\beta\right)+e^{Mh_2}\left(1+M\beta\right)\right)h_1+M\left(e^{Mh_1}\left(-1+M\beta\right)-e^{Mh_2}\left(1+M\beta\right)\right)h_2\right)\right)},$$

$$C_4 = \frac{\left(\begin{array}{l} e^{-3M(h_1+h_2)}(-4e^{3M(h_1+h_2)}FM^2\left(\begin{array}{l} e^{Mh_1}(1-M\beta)+ \\ e^{Mh_2}(1+M\beta)\end{array}\right)+e^{3M(h_1+h_2)}\left(e^{Mh_1}-e^{Mh_2}\right)^2 \\ \alpha\left(\begin{array}{l} 4e^{M(h_1+h_2)}M\beta+e^{2Mh_1}(-1+4M\beta) \\ +e^{2Mh_2}(1+4M\beta)\end{array}\right)B_1^3-\left(e^{Mh_1}-e^{Mh_2}\right)^2 \\ \alpha\left(\begin{array}{l} 4e^{M(h_1+h_2)}M\beta+e^{2Mh_1}(-1+4M\beta)+ \\ e^{2Mh_2}(1+4M\beta)\end{array}\right)B_2^3+6e^{3M(h_1+h_2)} \\ \alpha B_1^2B_2\left(\begin{array}{l} -e^{2Mh_1}+e^{2Mh_2}+2e^{2Mh_1}M\beta+2e^{2Mh_2}M\beta-4e^{M(h_1+h_2)} \\ M\beta+2e^{M(h_1+h_2)}Mh_1-2e^{M(h_1+h_2)}Mh_2\end{array}\right) \\ -6e^{2M(h_1+h_2)}\alpha B_1B_2^2\left(\begin{array}{l} -e^{2Mh_1}+e^{2Mh_2}+2e^{2Mh_1}M\beta+2e^{2Mh_2}M\beta \\ -4e^{M(h_1+h_2)}M\beta+2e^{M(h_1+h_2)}Mh_1-2e^{M(h_1+h_2)}Mh_2\end{array}\right)\end{array}\right)}{\left(4M\left(\begin{array}{l} -2e^{Mh_1}+2e^{Mh_2}+M\left(e^{Mh_1}(1-M\beta)+e^{Mh_2}(1+M\beta)\right)h_1 \\ +M\left(e^{Mh_1}(-1+M\beta)-e^{Mh_2}(1+M\beta)\right)h_2\end{array}\right)\right)},$$

REFERENCES

[1] Latham, T.W. (1966) Fluid motions in peristaltic pump (MS thesis). *MIT, Cambridge, MA.*

[2] Shapiro, A. H., Jaffrin, M. Y. and Weinberg, S. L. (1969) Peristaltic pumping with long wavelengths at low Reynolds number. *Journal of fluid mechanics,* 37(4), 799-825.

[3] Abdelsalam, S. I., & Vafai, K. (2017). Particulate suspension effect on peristaltically induced unsteady pulsatile flow in a narrow artery: blood flow model. *Mathematical biosciences*, *283*, 91-105.

[4] Kavitha, A., Reddy, R. H., Saravana, R., & Sreenadh, S. (2017). Peristaltic transport of a Jeffrey fluid in contact with a Newtonian fluid in an inclined channel. *Ain Shams Engineering Journal*, *8*(4), 683-687.

[5] Hussain, Q., Latif, T., Alvi, N., & Asghar, S. (2018). Nonlinear radiative peristaltic flow of hydromagnetic fluid through porous medium. *Results in Physics*, *9*, 121-134.

[6] Bhatti, M. M., Zeeshan, A., Ellahi, R., Bég, O. A., & Kadir, A. (2019). Effects of coagulation on the two-phase peristaltic pumping of magnetized Prandtl biofluid through an endoscopic annular geometry containing a porous medium. *Chinese Journal of Physics*, *58*, 222-234.

[7] Vaidya, H., Rajashekhar, C., Manjunatha, G., & Prasad, K. V. (2019). Peristaltic mechanism of a Rabinowitsch fluid in an inclined channel with complaint wall and variable liquid properties. *Journal of the Brazilian Society of Mechanical Sciences and Engineering*, *41*(1), 1-14.

[8] Rashid, M., Ansar, K., & Nadeem, S. (2020). Effects of induced magnetic field for peristaltic flow of Williamson fluid in a curved channel. *Physica A: Statistical Mechanics and its Applications*, *553*, 123979.

[9] Rajashekhar, C., Vaidya, H. Prasad, K. V. Tlili, I. Patil, A. and Nagathan, P. (2020) Unsteady flow of Rabinowitsch fluid peristaltic transport in a non-uniform channel with temperature-dependent properties. *Alexandria Engineering Journal*, 59(6), 4745-4758.

[10] Akram, J., Akbar, N. S. and Maraj, E. (2020) Chemical reaction and heat source/sink effect on magnetonano Prandtl-Eyring fluid peristaltic propulsion in an inclined symmetric channel. *Chinese Journal of Physics*, 65, 300-313.

[11] Abbas, Z., Rafiq, M. Y. Hasnain, J. and Javed, T. (2021) Peristaltic transport of a Casson fluid in a non-uniform inclined tube with Rosseland approximation and wall properties. *Arabian Journal for Science and Engineering*, 46(3), 1997-2007.

[12] Saleem, A., Akhtar, S. Alharbi, F. M. Nadeem, S. Ghalambaz, M. and Issakhov, A. (2020) Physical aspects of peristaltic flow of hybrid nano fluid inside a curved tube having ciliated wall. *Results in Physics*, 19, 103431.

[13] Akbar, Y. and Abbasi, F. M. (2020) Impact of variable viscosity on peristaltic motion with entropy generation. *International Communications in Heat and Mass Transfer*, 118, 104826.

[14] Abo-Elkhair, R. E., Bhatti, M. M. and Mekheimer, K. S. (2021) Magnetic force effects on peristaltic transport of hybrid bio-nanofluid (AuCu nanoparticles) with moderate Reynolds number: An expanding horizon. *International Communications in Heat and Mass Transfer*, *123*, 105228.

[15] Qureshi, I. H., Awais, M. Awan, S. E. Abrar, M. N. Raja, M. A. Z. Alharbi, S. O. and Khan, I. (2021) Influence of radially magnetic field properties in a peristaltic flow with internal heat generation: Numerical treatment. *Case Studies in Thermal Engineering*, 26, 101019.

[16] Abbas, Z. and Rafiq, M. Y. Analysis of heat and mass transfer phenomena in peristaltic transportation of hyperbolic tangent fluid in tapered channel. *Asia-Pacific Journal of Chemical Engineering*, e2675.

[17] Kumari, S., Rawat, T. K., & Singh, S. P. (2021). Modeling of nonlinear variable viscosity on peristaltic transport of fluid with slip boundary conditions: Application to bile flow in duct. *Journal of Scientific Research*, *13*(3), 821-832.

[18] Johnson Jr, M. W., & Segalman, D. (1977). A model for viscoelastic fluid behavior which allows non-affine deformation. *Journal of Non-Newtonian fluid mechanics*, *2*(3), 255-270.

[19] Hina, S., Hayat, T., & Alsaedi, A. (2012). Heat and mass transfer effects on the peristaltic flow of Johnson–Segalman fluid in a curved channel with compliant walls. *International Journal of Heat and Mass Transfer*, *55*(13-14), 3511-3521.

[20] Kothandapani, M., Prakash, J., & Pushparaj, V. (2016). Nonlinear peristaltic motion of a Johnson–Segalman fluid in a tapered asymmetric channel. *Alexandria Engineering Journal*, *55*(2), 1607-1618.

[21] Ashraf, H., Siddiqui, A. M., & Rana, M. A. (2018). Analysis of the peristaltic-ciliary flow of Johnson–Segalman fluid induced by peristalsis-cilia of the human fallopian tube. *Mathematical Biosciences*, *300*, 64-75.

[22] Hayat, T., Aslam, N., Khan, M. I., Khan, M. I., & Alsaedi, A. (2019). MHD peristaltic motion of Johnson–Segalman fluid in an inclined channel subject to radiative flux and convective boundary conditions. *Computer Methods and Programs in Biomedicine*, *180*, 104999.

[23] Rashid, M., Ansar, K. and Nadeem, S. (2020) Effects of induced magnetic field for peristaltic flow of Williamson fluid in a curved channel. *Physica A: Statistical Mechanics and its Applications*, 553, 123979.

[24] Akram, S., Athar, M. and Saeed, K. (2021) Hybrid impact of thermal and concentration convection on peristaltic pumping of Prandtl nanofluids in non-uniform inclined channel and magnetic field. *Case Studies in Thermal Engineering*, 25, 100965.

[25] Abbas, Z., Rafiq, M. Y. Hasnain, J. and Umer, H. (2021) Impacts of lorentz force and chemical reaction on peristaltic transport of Jeffrey fluid in a penetrable channel with injection/suction at walls. *Alexandria Engineering Journal*, 60(1), 1113-1122.

[26] Abbas, Z., Rafiq, M. Y. Alshomrani, A. S. and Ullah, M. Z. (2021) Analysis of entropy generation on peristaltic phenomena of MHD slip flow of viscous fluid in a diverging tube. *Case Studies in Thermal Engineering*, 23, 100817.

[27] Tanveer, A., Mahmood, S. Hayat, T. and Alsaedi, A. (2021) On electroosmosis in peristaltic activity of MHD non-Newtonian fluid. *Alexandria Engineering Journal*, 60(3), 3369-3377.

[28] Hayat, T., Nisar, Z. and Alsaedi, A. (2020) Impacts of slip in radiative MHD peristaltic flow of fourth grade nanomaterial with chemical reaction. *International Communications in Heat and Mass Transfer*, 119, 104976.

[29] Divya, B. B., Manjunatha, G. Rajashekhar, C. Vaidya, H. and Prasad, K. V. (2020) The hemodynamics of variable liquid properties on the MHD peristaltic mechanism of Jeffrey fluid with heat and mass transfer. *Alexandria Engineering Journal*, *59*(2), 693-706.

[30] Nisar, Z., Hayat, T. Alsaedi, A. and Ahmad, B. (2020) Significance of activation energy in radiative peristaltic transport of Eyring-Powell nanofluid. *International Communications in Heat and Mass Transfer*, 116, 104655.

[31] Imran, N., Javed, M. Sohail, M. and Tlili, I. (2020) Simultaneous effects of heterogeneous-homogeneous reactions in peristaltic flow comprising thermal radiation: Rabinowitsch fluid model. *Journal of Materials Research and Technology*, 9(3), 3520-3529.

[32] Alsaedi, A., Nisar, Z. Hayat, T. and Ahmad, B. (2021) Analysis of mixed convection and hall current for MHD peristaltic transport of nanofluid with compliant wall. *International Communications in Heat and Mass Transfer, 121*, 105121.

[33] Ibrahim, M. G., Hasona, W. M. and ElShekhipy, A. A. (2019) Concentration-dependent viscosity and thermal radiation effects on MHD peristaltic motion of Synovial Nanofluid: Applications to rheumatoid arthritis treatment. *Computer methods and programs in biomedicine*, 170, 39-52.

[34] Prakash, J., Siva, E. P. Tripathi, D. and Kothandapani, M. (2019) Nanofluids flow driven by peristaltic pumping in occurrence of magnetohydrodynamics and thermal radiation. *Materials Science in Semiconductor Processing*, 100, 290-300.

[35] Ahmed, B., Hayat, T. Abbasi, F. M. and Alsaedi, A. (2021) Mixed convection and thermal radiation effect on MHD peristaltic motion of Powell-Eyring nanofluid. *International Communications in Heat and Mass Transfer*, 126, 105320.

[36] Khazayinejad, M., Hafezi, M. and Dabir, B. (2021) Peristaltic transport of biological graphene-blood nanofluid considering inclined magnetic field and thermal radiation in a porous media. *Powder Technology*, 384, 452-465.

[37] Hayat, T., Iqbal, R. Tanveer, A. and Alsaedi, A. (2016) Influence of convective conditions in radiative peristaltic flow of pseudoplastic nanofluid in a tapered asymmetric channel. *Journal of Magnetism and Magnetic Materials*, 408, 168-176.

[38] Asha, S. K. and Deepa, C. K. (2019) Entropy generation for peristaltic blood flow of a magneto-micropolar fluid with thermal radiation in a tapered asymmetric channel. *Results in Engineering*, 3, 100024.

[39] Akram, S., Afzal, Q. and Aly, E. H. (2020) Half-breed effects of thermal and concentration convection of peristaltic pseudoplastic nanofluid in a tapered channel with induced magnetic field. *Case Studies in Thermal Engineering*, 22, 100775.

HEAT TRANSFER ANALYSIS OF JOHNSON-SEGALMAN FLUID IN TAPERED ASYMMETRIC CHANNEL

ORIGINALITY REPORT

17%	9%	16%	3%
SIMILARITY INDEX	INTERNET SOURCES	PUBLICATIONS	STUDENT PAPERS

PRIMARY SOURCES

1	Zaheer Abbas, Muhammad Yousuf Rafiq, Sabeeh Khaliq, Amjad Ali. "Dynamics of the thermally radiative and chemically reactive flow of Sisko fluid in a tapered channel", Advances in Mechanical Engineering, 2022 Publication	2%
2	M. Kothandapani, J. Prakash, V. Pushparaj. "Nonlinear peristaltic motion of a Johnson–Segalman fluid in a tapered asymmetric channel", Alexandria Engineering Journal, 2016 Publication	1%
3	Submitted to Higher Education Commission Pakistan Student Paper	1%
4	ihcoedu.uobaghdad.edu.iq Internet Source	1%
5	www.scipedia.com Internet Source	1%
	link.springer.com	